

5-1-2013

# Measurement of the Hydraulic Conductivity of Gravels Using a Laboratory Permeameter and Silty Sands Using Field Testing with Observation Wells

Aaron Judge

University of Massachusetts - Amherst, [judge@ecs.umass.edu](mailto:judge@ecs.umass.edu)

Follow this and additional works at: [http://scholarworks.umass.edu/open\\_access\\_dissertations](http://scholarworks.umass.edu/open_access_dissertations)

---

## Recommended Citation

Judge, Aaron, "Measurement of the Hydraulic Conductivity of Gravels Using a Laboratory Permeameter and Silty Sands Using Field Testing with Observation Wells" (2013). *Dissertations*. Paper 746.

This Open Access Dissertation is brought to you for free and open access by the Dissertations and Theses at ScholarWorks@UMass Amherst. It has been accepted for inclusion in Dissertations by an authorized administrator of ScholarWorks@UMass Amherst. For more information, please contact [scholarworks@library.umass.edu](mailto:scholarworks@library.umass.edu).

**MEASUREMENT OF THE HYDRAULIC CONDUCTIVITY OF GRAVELS  
USING A LABORATORY PERMEAMETER AND SILTY SANDS USING FIELD  
TESTING WITH OBSERVATION WELLS**

A Dissertation Presented

by

AARON JUDGE

Submitted to the Graduate School of the  
University of Massachusetts Amherst in partial fulfillment  
of the requirements for the degree of

DOCTOR OF PHILOSOPHY

May 2013

Civil and Environmental Engineering

© Copyright by Aaron Judge 2013

All Rights Reserved

**MEASUREMENT OF THE HYDRAULIC CONDUCTIVITY OF GRAVELS  
USING A LABORATORY PERMEAMETER AND SILTY SANDS USING  
FIELD TESTING WITH OBSERVATION WELLS**

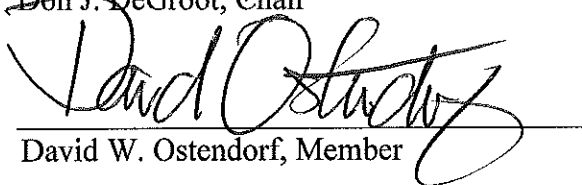
A Dissertation Presented

by

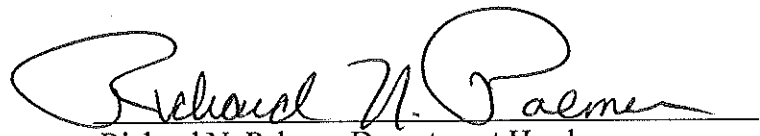
AARON JUDGE

Approved as to style and content by:

  
\_\_\_\_\_  
Don J. DeGroot, Chair

  
\_\_\_\_\_  
David W. Ostendorf, Member

  
\_\_\_\_\_  
David F. Boutt, Member

  
\_\_\_\_\_  
Richard N. Palmer, Department Head  
Civil and Environmental Engineering Department

## **DEDICATION**

To the late Professor Robert Campbell.

## ACKNOWLEDGMENTS

I thank my advisor Dr. Don DeGroot for teaching me so many skills over the many years I have had the pleasure of working with him. I have learned so many things from him such as ways of practically approaching problems and patiently learning to become a better writer by reading and presenting my work to so many people. He also gave me the pleasure of working with the environmental engineering group many years ago which has been a great experience for me. I thank Dr. David Ostendorf for teaching me how to model the data we geotechs measure so well. I also learned to write and present my results much better to audiences of all kinds as a direct result of working with him. When my first paper was accepted, I thought of him when I made a fist pump because I thought of how much he pushed me to get it right. I also thank him for providing funding for me ever since I was an undergrad in 2004. I thank Dr. David Boutt for serving on my committee; it is great to have my work approved by a geologist with a hydrogeology background. I eagerly await to see his contributions to my dissertation so I can clearly reach out to a larger audience with my work. I also thank Dr. Vitaly Zlotnik for being an author on my first manuscript. His valuable work helped my first paper get accepted, and I expect the same will come from Dr. Boutt's contributions on the second and third papers.

I thank fellow grad students, most notably Phil Dunaj who passed the torch of the salt project to me, Dr. Melissa Maynard, Patty Kral, and Laura Carey who I had the pleasure to do research with, and Will Lukas who is receiving the torch of the salt project. It has been a pleasure to work with them and all other students in the geotechnical engineering program. I also learned programming skills from Dr. Camelia Rotaru and

practical approaches to problem solving from Dr. Erich Hinlein in the environmental engineering program. I also thank my mother, father, stepmother, and sister Amy who have always been so very supportive of the work I have done over the years. I also thank Jeremy Gummesson for hundreds of trips to the campus center for coffee on long days and all other friends as well.

Finally, I would like to acknowledge the Massachusetts Department of Transportation for funding this project under Interagency Service Agreement No. 73140 with the University of Massachusetts Amherst. The views, opinions, and findings contained in this thesis do not necessarily reflect Massachusetts Department of Transportation official views or policies. This thesis does not constitute a standard, specification, or regulation.

## **ABSTRACT**

MEASUREMENT OF THE HYDRAULIC CONDUCTIVITY OF GRAVELS USING A  
LABORATORY PERMEAMETER AND SILTY SANDS USING FIELD TESTING  
WITH OBSERVATION WELLS

MAY 2013

AARON JUDGE, B.S., UNIVERSITY OF MASSACHUSETTS AMHERST

M.S., UNIVERSITY OF MASSACHUSETTS AMHERST

Ph.D., UNIVERSITY OF MASSACHUSETTS AMHERST

Directed by: Professor Don J. DeGroot

A new laboratory permeameter was developed for measuring the hydraulic conductivity of gravels ranging from 0.1 to 2 m/s. The release of pneumatic pressure applied to the test specimen induces an underdamped oscillatory response of the water level above the permeameter, similar to an underdamped in situ slug test response in monitoring wells. A closed form model was derived to calibrate the hydraulic minor losses in the permeameter and the hydraulic conductivity of the specimen by performing tests without and with a specimen. The majority of each test series performed on individual specimens produced hydraulic conductivity values within 10% of the average, which is very small for such a measurement.

Tests were performed using the permeameter on a collection of subrounded and angular gravels prepared to measured grain size distributions and porosities. The surface area was determined by evaluating the shape and angularity using a method developed in this research and these parameters were used with the measured tortuosity and hydraulic



conductivity, to back calculate the packing factor of the Kozeny-Carman equation. The results show that the packing factor for the gravels and materials tested is proportional to the tortuosity cubed. These results provide a valuable update to the Kozeny-Carman equation for predicting the hydraulic conductivity of gravels.

Field slug interference tests were performed in pairs of monitoring wells installed at the same elevation in a floodplain deposit of silty sand in Dedham MA. Slug tests were performed in one of the wells while the response was monitored simultaneously in both wells. The measured responses were both analyzed by modifying the KGS model of Hyder et al. (1994) to consider the wellbore storage and filter packs effects. This modification was found to produce estimates of hydraulic conductivity based on the slugged well response that compared well with that estimated based on the observation well's response. Calibrated hydraulic conductivities for the pairs of wells tested ranged from  $4 \times 10^{-6}$  to  $1.5 \times 10^{-5}$  m/s and specific storage ranged from  $2 \times 10^{-5}$  to  $7 \times 10^{-4}$  m<sup>-1</sup>.

	Page
ACKNOWLEDGMENTS .....	v
ABSTRACT.....	vii
LIST OF TABLES.....	xi
LIST OF FIGURES .....	xii
LIST OF SYMBOLS .....	xiii
 CHAPTER	
1 INTRODUCTION .....	1
2 A PNEUMATIC PERMEAMETER FOR TRANSIENT TESTS ON COARSE GRAVEL.....	5
2.1 Introduction.....	6
2.2 Methods.....	11
2.3 Materials tested .....	14
2.4 Theory .....	15
2.4.1 Conservation of Momentum .....	15
2.4.2 Minor Losses.....	20
2.4.3 Linearization .....	21
2.4.4 Governing Equation and Oscillation Frequency.....	22
2.4.5 Minor Loss Calibration .....	23
2.4.6 Hydraulic Conductivity Calibration.....	25
2.5 Results.....	26
2.6 Conclusions.....	30
3 USING THE KOZENY-CARMAN EQUATION TO PREDICT THE PERMEABILITY OF GRAVELS.....	32
3.1 Introduction and background .....	32
3.2 Tests performed and procedures .....	37
3.2.1 Porosity and tortuosity .....	37
3.2.2 Grain size distribution.....	40
3.2.3 Soil grain shape.....	41

3.2.4	Calculation of grain angularity and surface area using perimeter measurements .....	44
3.2.5	Packing factor .....	46
3.3	Results.....	47
3.4	Conclusions.....	49
4	SLUG INTERFERENCE TESTS CONSIDERING THE EFFECTS OF WELLBORE STORAGE IN THE TESTED AND OBSERVATION WELLS .....	52
4.1	Introduction and background .....	52
4.2	Model and boundary value problem .....	56
4.2.1	Analytical model of slug interference tests.....	57
4.3	Site description and well arrangement.....	60
4.3.1	Methods of performing tests .....	62
4.3.2	Results.....	62
4.4	Discussion.....	65
4.5	Summary and Conclusions .....	67
5	SUMMARY AND CONCLUSIONS .....	68
	APPENDIX: LIST OF PRESENTATIONS .....	70
	BIBLIOGRAPHY.....	87

## LIST OF TABLES

Table	Page
2.1: Results of tests .....	25
2.2: Statistics of calibrations .....	30
2.3: Reynolds number comparison .....	30
3.1: Permeability predictions and soil parameters using the Kozeny Carman equation with the packing factor as described in Equation 3.17 with $\eta$ = 3. ....	47
3.2: Comparison of the effects of parameters on the permeability .....	49
4.1: Dimensions of the wells and hydraulic conductivity based on previous slug tests by LaMesa (2008).....	61
4.2: Slug test calibrations determined considering the presented model using Equation 4.12 for both wells and the other equations for the observation well. ....	63
4.3: Slug test results from LaMesa (2008) using the Bouwer and Rice method .....	63

## LIST OF FIGURES

Figure	Page
2.1: Schematic diagram of the permeameter.....	13
2.2: Materials tested.....	15
2.3: Grain size distribution of materials tested and from other sources with relevant results ( $K_{10}$ is used where the tested temperature is known).....	15
2.4: Pressure fluctuations (circles) and calibrations (lines) from the static value ( $D_T$ ).....	25
3.1: Grain Size Distribution of the Brown Stone (BS) and Tap Rock (TR). Tap Rock is shown in the left of the photograph and Brown Stone is shown in the right.....	36
3.2: Measured and calibrated pressure head for the Brown Stone small well graded specimen.....	39
3.3: Tortuosity through a specimen of soil (from Fair and Hatch (1933)).....	40
3.4: The effects of angularity and shape on the shape factor ( $C_{SH}$ ) and a comparison of the measured axes vs. the equivalent axes and their effect on the volume factor ( $C_V$ ).....	43
3.5: Surface area vs. effective diameter for the grain sizes considered.....	45
3.6: Predicted vs. measured permeability using Equation 3.1 and 3.17.....	51
4.1: Definition Sketch.....	55
4.2: Dedham site location from LaMesa (2008).....	61
4.3: Slug test results in the slugged and observation wells using the model presented in Equation 4.12 for the observation wells.....	64
4.4: The three observation well models considered in Table 4.2 using the hydraulic conductivity and specific storage values calibrated using Equation 4.12.....	66

## LIST OF SYMBOLS

Symbol	Units	Description
$A_B$	$m^2$	area of the three base holes
$A_C$	$m^2$	area of the cylinder
$A_P$	$m^2$	porous area of specimen
$A_R$	$m^2$	riser area
$D_T$	m	depth to transducer
$d_x$	m	diameter with x% passing
$F_B$		minor loss in the base
$F_P$		sum of minor losses in the system
$F_R$		minor loss in the riser
$g$	$m/s^2$	gravitational acceleration
$h_B$	m	head loss at the base of the permeameter
$h_R$	m	head loss at the bottom of the riser
Hz	$s^{-1}$	Hertz
$k$	$m^2$	specimen permeability
$K$	m/s	hydraulic conductivity

$K_{10}$	m/s	hydraulic conductivity at 10 degrees Celsius
$L_C$	m	length of the cylinder
$L_E$	m	effective riser length
$L_R$	m	length of riser
$L_S$	m	length of the top of cylinder
$N$		number of observations considered in each test
$n$		porosity
$P$	kPa	pressure change at the transducer elevation
$p$	kPa	pressure at elevation $z$
$p_C$	kPa	calibrated pressure
$p_T$	kPa	transducer pressure
$p_Z$	kPa	pressure at elevation $z$ outside the permeameter
$t$	s	time
$t_C$	s	characteristic time duration
$w_A$	m/s	average characteristic velocity in the riser
$w_B$	m/s	velocity in the base
$w_C$	m/s	velocity in the cylinder

$w_R$	m/s	velocity in the riser
$z$	m	elevation above the datum
$z_0$	m	static free surface elevation
$z_B$	m	elevation at the base
$z_R$	m	riser bottom elevation
$z_T$	m	transducer elevation
$\delta$		error
$\eta$	m	position of the water level above the free surface
$\nu$	$m^2/s$	water kinematic viscosity
$\rho$	$kg/m^3$	water density
$\tau$		tortuosity
$\omega$	$s^{-1}$	frequency
$a$	m	adjusted a axis
$a_m$	m	measured a axis
$b$	m	adjusted b axis
$b_m$	m	measured b axis
$c$	m	adjusted c axis



$c_m$	m	measured c axis
$C_{PK}$		packing factor
$C_{SA}$		surface area factor
$C_{SH}$		shape factor
$c_v$		volume constant
$d_{eff}$	m	effective diameter
$d_l$	m	larger diameter
$d_s$	m	smaller diameter
$g$	$m/s^2$	gravity
$h_0$	m	initial pressure head during a test
$h(t_c)$	m	pressure head during a test at a characteristic time
$t_c$	s	characteristic time
$K$	m/s	hydraulic conductivity
$k$	$m^2$	permeability
$k_m$	$m^2$	permeability measured from a test
$k_p$	$m^2$	permeability predicted using Kozeny-Carman equation
$L_S$	m	specimen length

$m_G$	kg	grain mass
$m_T$	kg	total mass
$n$		porosity
$p$		mathematical constant
$P$	m	perimeter of grain
$P_e$	m	perimeter of an ellipse
$SA$	$m^2$	surface area determined from AutoCAD
$SA_e$	$m^2$	surface area of an ellipse
$SA_G$	$m^2$	surface area per gram
$V_G$	$m^3$	volume of grain
$V_S$	$m^3$	volume of solids
$\delta$		factor (error)
$\eta$		exponent of tortuosity
$\lambda$	m	length traveled by water
$\rho_s$	$kg/m^3$	density of solids
$\tau$		tortuosity
$\nu$	$m^2/s$	kinematic viscosity

$C_{DS}$		wellbore storage factor in the slugged well
$C_{DO}$		wellbore storage factor in the observation well
$h$	m	hydraulic head in the aquifer
$h^*$	m	transformed hydraulic head in the aquifer
$h_i$	m	initial head in the aquifer
$H_0$	m	applied slug
$h_{OB}$	m	hydraulic head in the observation well
$h_{OB}^*$	m	transformed hydraulic head in the observation well
$h_{SL}$	m	head in the slugged well
$h_{SL}^*$	m	transformed hydraulic head in the slugged well
$K$	m/s	hydraulic conductivity of the formation
$K_0$		Modified Bessel function of the zero order
$K_1$		Modified Bessel function of the first order
$K_{SK}$	m/s	hydraulic conductivity of the skin
$k$	$m^2$	soil permeability
$L_S$	m	length of the screen
$L_{SK}$	m	length of the skin

$n$		porosity
$p$		LaPlace transform coefficient
$Q$	$\text{m}^3/\text{s}$	flow into the well
$r$	$\text{m}$	radial distance from the centerline of the well
$r_c$	$\text{m}$	radius of the riser casing
$r_D$		dimensionless radial distance $r/r_c$
$r_{SK}$	$\text{m}$	radius of the skin
$S$	$\text{m}^{-1}$	specific storage of the soil
$t$	$\text{s}$	time
$z$	$\text{m}$	elevation above the impermeable bottom of the deposit
$\xi_1$		first coefficient of Equation 4.10
$\xi_2$		second coefficient of Equation 4.10
$\Omega_1$		first coefficient of Equation 4. 9
$\Omega_2$		second coefficient of Equation 4.9
$\alpha$	$\text{Pa}^{-1}$	compressibility of soil
$\beta$	$\text{Pa}^{-1}$	compressibility of water
$\rho_w$	$\text{kg}/\text{m}^3$	density of water

# CHAPTER 1

## INTRODUCTION

Gravels are extensively used in roadway construction, drainage curtains, and railroad ballast which fouls over time, affecting the hydraulic conductivity. In some projects the gravel must be able to provide a minimum and high enough rate of drainage and engineers and contractors are required to prove that their source material or an existing material has a high enough hydraulic conductivity via direct measurement to satisfy this. Open-framework gravel can be found in gravelly fluvial deposits interstratified with sand and gravel as well as in glaciofluvial aquifers. The hydraulic conductivity of gravel is difficult to test because laboratory tests usually do not provide laminar flow and wells are not commonly installed in gravel formations. Chapuis and Aubertin (2003) noted that the accuracy of laboratory permeability tests (e.g., ASTM 2002) in coarse grained materials is often questionable; they note that laboratory hydraulic conductivity values from just three replicate tests may vary broadly.

The Kozeny-Carman equation is the most accurate grain size model for estimating hydraulic conductivity because it considers the porosity and surface area of the soil. The packing factor was empirically determined by Carman (1956) to be equal to 5 for uniform spheres, and this value has been used since then. The tortuosity squared was suggested to be considered in the denominator of the Kozeny-Carman Equation by Scheidegger (1957), Costa (2006) and a few others, though it has been rarely evaluated and used. Furthermore, if the roundness and angularity were estimated by a method of determining the shape factor, the formula would provide better accuracy (Carman 1956). If more accurate soil properties were used then the Kozeny-Carman equation would predict values with better accuracy. Chapuis and Aubertin (2003) considered the distribution of

grain sizes and found the Kozeny-Carman results to be within a factor of three of the measured results for soils where the permeability ( $k$ ) ranges over orders of magnitude. The accuracy and precision of the measured  $k$  and grain size distribution values of the tests they considered were unknown, and are very likely less than satisfactory in some cases, especially for soils with high  $k$ .

Slug testing is the most common method used to determine a quick estimate of the in situ hydraulic conductivity of a deposit. Uncertainty of soil, formation, and well properties provide different hydraulic properties for any analysis. Results are sometimes fit to type curves that are a function of hydraulic conductivity and specific storage and often times the data are forced to fit a curve that is compromised. Misinterpretation of the initial displacement of water is another reason that results may differ. The wellbore storage (water in the open well) and the wellskin (water in the highly permeable filter pack) are not always considered in slug tests. Different methods of analysis provide results within about a half an order of magnitude of error, showing that either not everything is being considered in all solutions, or that some assumptions are wrong. Analyzing slug tests performed in a pair of wells installed at the same elevation and close to each other horizontally while measuring the hydraulic response, provides data for analysis that eliminates some of this uncertainty.

The primary objective of this dissertation was to find better ways to evaluate hydraulic conductivity of highly permeable coarse grained soils using a new laboratory device, as well as an improved method of analyzing slug interference tests. The tasks performed to meet this goal were to:

1. Design and build a new permeameter for performing quick laboratory tests on gravels with hydraulic conductivity values ranging from 0.1 to 2 m/s.
2. Develop a model to calibrate the hydraulic conductivity using this new device while proving that the results are repeatable, consistent, and follow Darcy's law.
3. Show that the Kozeny-Carman Equation works for spheres tested because it is well established for spheres.
4. Use the Kozeny-Carman Equation for other types of tested coarse grained soils that are commonly found as well as anisotropic stones that allow the tortuosity to be calibrated in the model of Judge et al. (*in press*).
5. Modify the Kozeny-Carman Equation to include the tortuosity on these gravels as well as other soils since it is known that it has an influence but has not been tested experimentally.
6. Perform slug interference tests utilizing two wells with one test and one model. This eliminates many of the errors that are seen in slug tests, mainly because they both test a similar volume of soil at the same time.
7. Consider the wellbore storage (water in the open well) and wellskin (well filter pack) in both wells for interpretation of the slug interference tests because they both can have a strong influence on the results.

Chapters 2 to 4 present the results of this research and Chapter 5 presents a summary and conclusions. Chapter 2 presents the results of the development of a permeameter for transient tests on gravels as well as a model to calibrate the hydraulic conductivity using this device. It is the second of its kind, following Ferrierra et al. (2010), but has a few more advantages such as rapid testing and it provides tortuosity

estimates. This work has been accepted for publication: Judge, A.I., Ostendorf, D.W., DeGroot, D.J. and Zlotnik, V.A. (*in press*). “A Pneumatic Permeameter for Transient Laboratory Tests.” *Journal of Hydrologic Engineering*.

Chapter 3 presents results from tests performed using the new permeameter described in Chapter 2 by considering soils of different shapes and gradation. The data were used to develop an experimentally calibrated packing factor for the Kozeny-Carman Equation as a function of tortuosity using the measured hydraulic conductivity. This chapter was prepared in the form of a manuscript that has been prepared for submission to a peer-reviewed journal.

Chapter 4 presents the results of slug interference tests performed in pairs of wells in a silty sand floodplain deposit to evaluate the hydraulic conductivity and specific storage. The wellbore storage and wellskin were found to have strong effects on interpretation of the results, something that is typically not considered using current methods. This chapter was prepared in the form of a manuscript that has been prepared for submission to a peer-reviewed journal.

The Appendix contains slide posters and presentations of meetings and conferences attended during the time of this study.



## CHAPTER 2

### A PNEUMATIC PERMEAMETER FOR TRANSIENT TESTS ON COARSE GRAVEL

A new permeameter is proposed for performing laboratory hydraulic conductivity tests on gravels with hydraulic conductivity values ranging from 0.1 to 1 m/s. A small diameter riser is connected to a large diameter cylinder, which holds the coarse-grained specimen saturated in a water bath. The release of pneumatic pressure applied to the free surface in the riser induces an underdamped oscillatory response of the water level in the riser, similar to an underdamped in situ slug test response in monitoring wells. A closed form model used to analyze the measured oscillatory hydraulic head data to calibrate the minor losses in the permeameter and the hydraulic conductivity of the specimen by performing tests without and with a specimen. The average model error of calibrated pressure head values in the riser for the tests considered is on the order of 5% of the initial displacement of about 2 cm. The hydraulic conductivity values are calibrated considering replicate tests, tests of different specimen lengths, and different time periods within a test to verify that the results reflect the hydraulic conductivity of the specimen alone. The Kozeny-Carman equation which considers the specific surface area of the tested material gave a hydraulic conductivity value within 5% of the measured value for the marbles, which is a good comparison because the uniform marbles have a known specific surface area. For all the various tests performed on each specimen, most of the hydraulic conductivity values were within 10% of the average, while the specimens with hydraulic conductivity greater than 1 m/s were within 10 to 20% of the average.

## 2.1 Introduction

A new permeameter is proposed for performing laboratory hydraulic conductivity tests on gravels with hydraulic conductivity values ranging from 0.1 to 1 m/s. A small diameter riser is connected to a large diameter cylinder, which holds the coarse-grained specimen saturated in a water bath. The release of pneumatic pressure applied to the free surface in the riser induces an underdamped oscillatory response of the water level in the riser, similar to an underdamped in situ slug test response in monitoring wells. A closed form model used to analyze the measured oscillatory hydraulic head data to calibrate the minor losses in the permeameter and the hydraulic conductivity of the specimen by performing tests without and with a specimen. The average model error of calibrated pressure head values in the riser for the tests considered is on the order of 5% of the initial displacement of about 2 cm. The hydraulic conductivity values are calibrated considering replicate tests, tests of different specimen lengths, and different time periods within a test to verify that the results reflect the hydraulic conductivity of the specimen alone. The Kozeny-Carman equation which considers the specific surface area of the tested material gave a hydraulic conductivity value within 5% of the measured value for the marbles, which is a good comparison because the uniform marbles have a known specific surface area. For all the various tests performed on each specimen, most of the hydraulic conductivity values were within 10% of the average, while the specimens with hydraulic conductivity greater than 1 m/s were within 10 to 20% of the average.

Gravels are extensively used in roadway construction, in drainage curtains, and railroad ballast which fouls over time, affecting the hydraulic conductivity. In some projects the gravel must be able to provide a minimum and high enough rate of drainage

and engineers and contractors are required to prove that their source material or an existing material has a high enough hydraulic conductivity via direct measurement to satisfy this. Open-framework gravel can be found in gravelly fluvial deposits interstratified with sand and gravel as well as in glaciofluvial aquifers. Cedergren (1977) showed an example where lenses of open-framework gravel with  $K$  was 0.3 m/s within silt where  $K$  was  $10^{-4}$  m/s resulted in over five orders of magnitude more seepage under a dam. The high permeability of open-framework gravel strata is due to the lack of sediment blocking pore space between gravel grains. Ferreira et al. (2010) noted that these zones of high permeability ( $K = 0.04$  m/s) form preferential flow pathways which can act as “thief zones” during the recovery of reservoirs. Bobo and Khoury (2012) collected samples in Prince William Sound, Alaska and used a capillary model and the Kozeny-Carman equation to determine the hydraulic conductivity at a tidally induced beach where  $K$  was estimated (i.e., not directly measured), to be 0.01 m/s near the beach surface. Bobo and Khoury (2012) noted that the hydraulic conductivity of the gravel at the beach surface plays a critical role in the lag of water table fluctuations behind tidal oscillations.

Chapuis and Aubertin (2003) noted that the accuracy of laboratory permeability tests (ASTM 2002) in coarse grained materials is often questionable; they note that laboratory hydraulic conductivity values from just three replicate tests may vary broadly. This lack of precision partially depends on test equipment and procedures and also due to the natural variability of the tested material. Constant-head and falling-head laboratory tests are commonly used to determine the saturated permeability ( $k$ ) or hydraulic conductivity ( $K$ ) of coarse-grained materials. Constant-head tests using a Marriott tube

are used for coarse-grained soils with high  $K$  values because it supports a small head difference over the specimen, which is critical for preventing non-Darcian (turbulent) effects. Frequent readings of the water level must be taken and an accurate and truly constant head must be applied. In the common constant head equipment set up that uses a Mariott tube to maintain constant head pressure, both of these factors are complicated by the lack of clean and quick release of air bubbles from the bottom of the bubble tube.

Flow through a specimen is proportional to the gradient as long as the flow is laminar, or Darcian. Lambe and Whitman (1969) stated that the critical Reynolds number above which flow is not laminar and Darcy's law is no longer valid should be determined experimentally for soils that are more permeable than medium sand. Scheidegger (1957) stated that the critical Reynolds number ranges from 0.1 to 75 with higher Reynolds numbers for larger grain sizes. Theoretically the Reynolds number is about 2,000 for flow through straight tubes but pore spaces in soils are far from straight and this number should be adjusted by multiplying by the porosity and divided by three because the water can move in three spatial directions which yields a critical Reynolds number of about 250 to 300 for typical values of porosity for gravels. Identical Reynolds numbers are not sufficient to compare dynamic similarities between specimens (Cedergren 1977), who report data giving a Reynolds number of 150 for constant head tests performed on coarse gravel up to 4 cm in diameter.

Performing laboratory tests to directly measure the hydraulic conductivity of gravels is limited, likely in part due to the difficulties in conducting such tests as noted above. However, Ferreira et al. (2010) recently developed the "megapermeameter" for testing of gravels with a specimen length of 3 meters and diameter of 10 cm. Small heads

(on the order of 0.1-1.0 cm) were measured to a resolution of  $10^{-5}$  m to maintain the laminar flow regime which was determined by performing tests at varying gradients and noting when the gradient was no longer proportional to the velocity. Each test required a permeation period of 3 hours to 3 days to ensure flow stabilization. Uniform pebbles with a diameter of 1 cm were used to proof test the equipment and yield  $K$  equal to 1.0 m/s which was equal to the values of the Kozeny-Carman equation. The flow was increased slowly until it was no longer laminar which was found to be at a critical Reynolds number of 25 for the pebble specimens and 10 for the open-framework gravel. Data collected at higher Reynolds numbers yielded erroneously low  $K$  values.

Plain and Morrison (1953) performed experiments on spherical glass beads with diameters of 0.016 cm to 0.3 cm using water and a silicone fluid with a much lower viscosity and a constant flow rate for all tests. These tests with varying viscosities yielded a critical Reynolds number for given grain sizes which was 100 when water was used on the glass beads with a small diameter size of 0.13 cm while it was lower for specimens with a smaller diameter. Tennakoon et al. (2012) tested clean and fouled ballast (2 to 5 cm diameter) stating that the flow was laminar because a gradient less than four was used and  $K$  was found to be 0.3 m/s using a standard constant head permeameter. However, a back calculation of the Reynolds number based on their data indicates that the Reynolds number appears to be at least 10,000, and thus the flow region was very likely nonlaminar. White et al. (2007) developed an in situ air penetrometer for testing of granular bases as permeable as 0.1 m/s. The test was primarily developed to improve values used for drainage coefficients and to evaluate potential variability of the

gradation of the source material. The results were found to not be very consistent and were up to five times higher than compaction mold permeameter tests.

Grain size models and constant head tests are the only current way to test soils more permeable than 0.01 m/s unless a well is installed in the field in such a deposit where a slug test can be performed using pneumatic methods. The falling-head test fails to give reliable  $K$  values for gravels because water level responses in coarse specimens may be turbulent and inertial (depending on the equipment set up used), which cannot be evaluated using the falling head equation. The oscillatory response of slug tests performed in wells where  $K$  is high has been observed and studied by Butler (1997) and Ostendorf et al. (2005). The period of the oscillations in a well is governed by the inertia of the water column (e.g., Zlotnik and McGuire (1998) and Zurbuchen et al. (2002)), which is calculated considering the geometry of the flow system. An analogous phenomenon would occur in a laboratory permeameter, with an appropriate geometry and equipment set-up, where the underdamped response would be dampened by the  $K$  of the specimen and head losses in the permeameter. Any head losses that may occur due to contractions in the permeameter, if they exist, can be incorporated with the closed form model using the same approach of Zlotnik and McGuire (1998) and Ostendorf et al. (2005) for in situ slug tests and for which head losses due to contractions and friction in the riser were considered.

This paper describes a new laboratory permeameter and a corresponding closed form theory for testing the hydraulic conductivity of coarse grained soils such as gravels. A significant objective of the work was to develop an alternative equipment set up and test procedure than the megapermeameter developed by Ferreira et al. (2010). The

permeameter described in the paper uses a much shorter test specimen and a much shorter test period than the three meter tall specimen and 3 hours to 3 day test period of Ferreira et al. (2010). The equipment was designed to improve upon the challenge of performing traditional constant head tests on highly permeable soils such as gravels. The hydraulic response in the new permeameter is underdamped and the oscillatory signal is interpreted using a modified form of the model of Ostendorf et al. (2005) to determine the hydraulic conductivity. The modifications consider that the flow in the permeameter is vertical, that there is a smaller diameter riser above the specimen, and that flow exits and enters the region below the bottom of the specimen chamber horizontally. Minor losses are calibrated to the measured water pressure in the riser for tests performed without a specimen, and then those values are used to calibrate  $K$  to the measured water pressure in the riser for tests performed with a specimen. This method is illustrated for various coarse-grained specimens where the oscillation amplitudes decay more rapidly with less permeable specimens. The specimen length and applied pressure head are varied, and results obtained for perfect spheres (marbles) are compared with the Kozeny-Carman hydraulic radius model to verify that the results yield accurate and precise  $K$  values.

## **2.2 Methods**

A cylindrical permeameter made of PVC with a diameter of 15 cm and an adjustable specimen length of up to 25 cm has one screen near the bottom where the specimen is held as shown in Figure 2.1. The screen holding the specimen is made of stainless steel woven wire cloth Type 304 with porosity of 0.58, opening square length of 1.9 mm, and wire diameter of 0.6 mm. The permeameter is placed in a barrel (0.4 m in diameter and 0.5 m tall), which acts as a water bath keeping the static water level 0.4 m

above the holes in the base of the cylinder. The permeameter is airtight and watertight; a manifold at the top allows pressure transducers and cables to pass through a port using a split rubber plug inside of a compressible ring (Ostendorf et al., 2005) to measure the pressure of the air and the water in the riser.

The manifold with a 5 cm ball valve is connected to the top of the riser to hold the water level at the desired level. Pneumatic pressure of about 200 to 300 Pa is applied to the free surface of the water through the manifold using a quick-connect pneumatic fitting, which depresses the free surface of water in the riser by 2 to 3 cm. The test is then commenced by opening the valve, which instantly allows water to flow through the permeameter and into and out of the water bath which has an area large enough relative to the small volume of water displaced to keep a quasi-static water level during the tests. Another advantage of having a specimen area larger than the riser is that the velocity of the water flowing through it is lower, keeping it laminar.

One transducer measures the air pressure above the water and the other is lowered to a depth of 5 to 10 cm in the riser below the static water level at an elevation where it is stays submerged. The applied pressure and the water pressure in the riser are measured using vented pressure transducers at a frequency of 100 Hz, because the period of the water level fluctuations occur over one second for all of the tests performed. This system consists of a National Instruments modular signal conditioning module and a National Instruments PC card 16 bit multifunction I/O analog to digital converter processed the signal, and a laptop using LabView to save the data (Ostendorf et al., 2007).



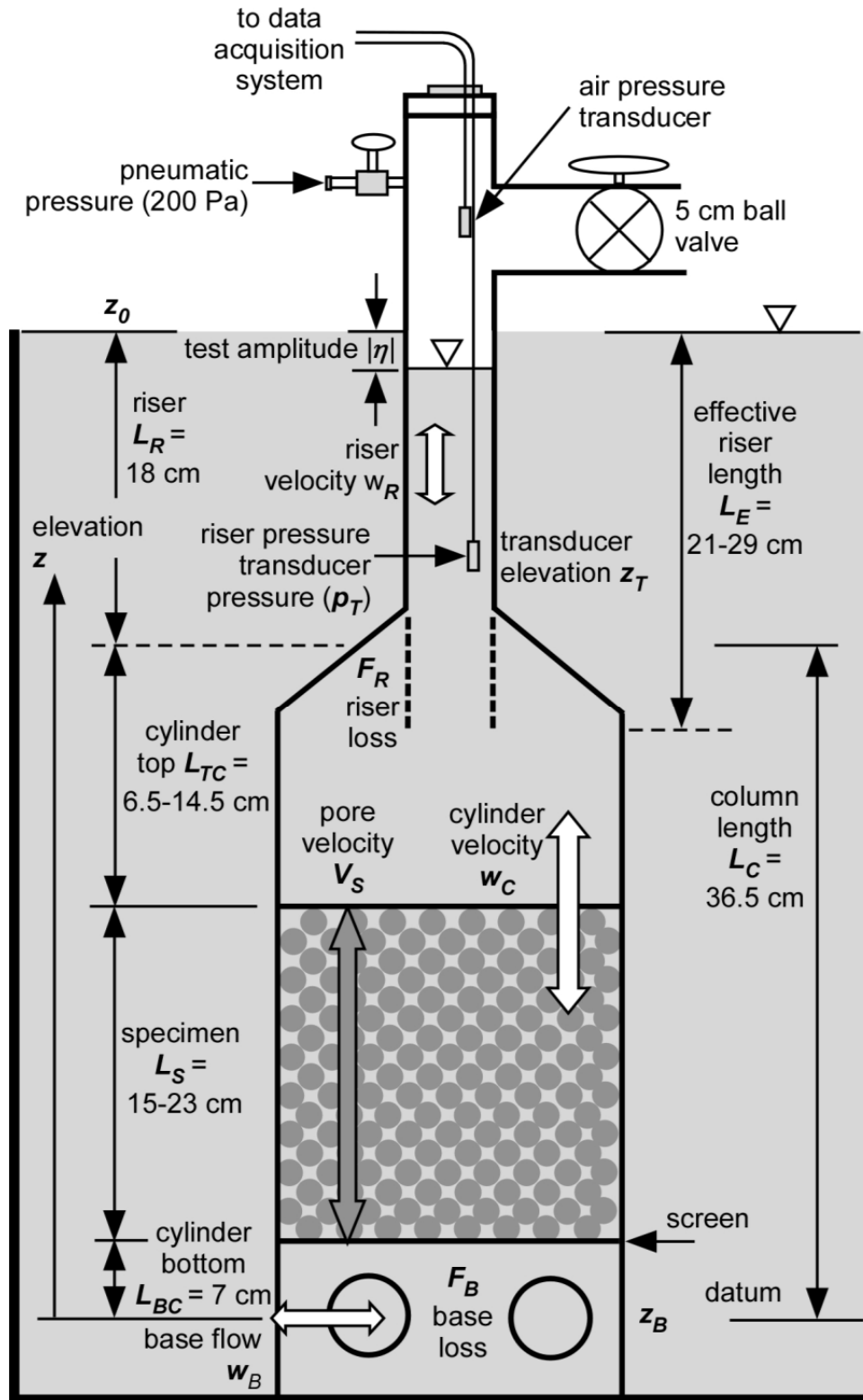


Figure 2.1: Schematic diagram of the permeameter.

### 2.3 Materials tested

Figure 2.2 shows the test materials and Figure 2.3 presents the corresponding grain size distribution curves. These materials include fine to very coarse gravels including oblong stones which were tested with the long axis aligned with the vertical flow direction (V Stones) and horizontal (H Stones). Although the volumetric void ratios and grain size distributions of the stones are identical, the tortuosity of the flow of water is greater for the horizontally aligned specimens, resulting in a lower permeability.

Marbles with a uniform diameter of 1.5 cm were tested to compare with that predicted by the Kozeny-Carman equation which considers the void ratio, specific surface area, and packing factor, which is easy to compute for uniform spherical marbles unlike that for natural soils. Chapuis and Aubertin (2003) evaluated the Kozeny-Carman model by studying literature results for laboratory measurement of the hydraulic conductivity of a large variety of grain size distributions and void ratios. Rather than using one effective diameter, they considered the distribution of grain sizes and found the Kozeny-Carman results to be within a factor of three of the measured results for soils where the hydraulic conductivity was less than 0.01 m/s. The observed discrepancies were attributed to practical reasons such as inaccurate surface area values, unsteady flow or unsaturated specimens. Theoretical reasons may also include anisotropy, motionless water in the specimens, or erroneous packing and roundness coefficients.

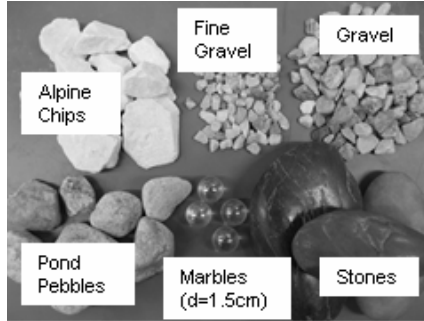


Figure 2.2: Materials tested

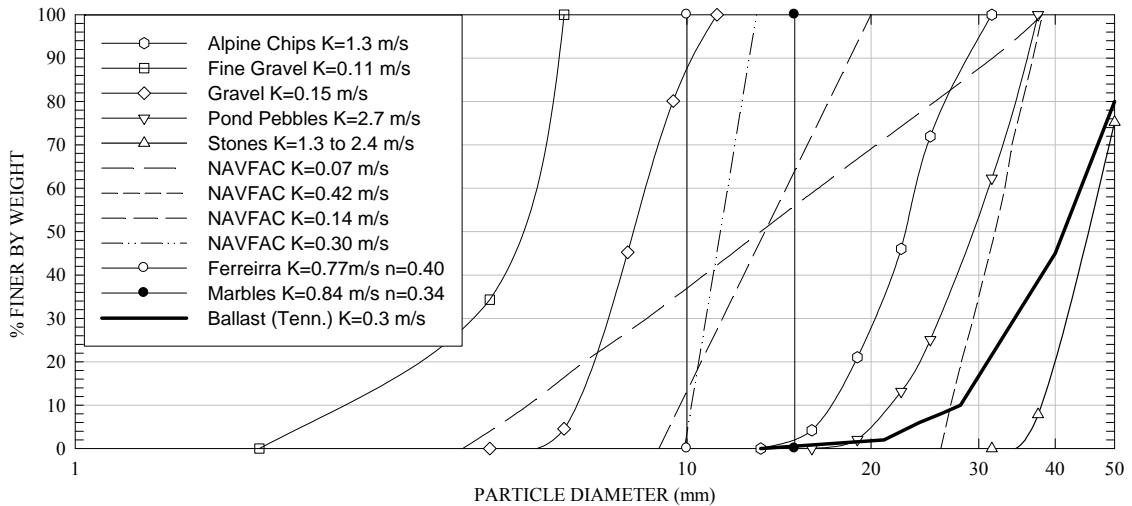


Figure 2.3: Grain size distribution of materials tested and from other sources with relevant results ( $K_{10}$  is used where the tested temperature is known)

## 2.4 Theory

### 2.4.1 Conservation of Momentum

Figure 2.1 illustrates the permeameter highlighting the concepts, geometrical parameters, flow direction, and origin of z-coordinate. Head losses occur at the contractions at the base and riser bottom and there is friction over the length of the specimen when water flows in and out of the permeameter. The vertical pressure gradient in the reservoir outside of the permeameter is hydrostatic, while it is both inertial and hydrostatic inside. The inertial effects are calculated considering the velocity over

the four different vertical regions effects and are summed as the effective riser length ( $L_E$ ) to calibrate  $k$  to the water level change during the tests. The specimen length ( $L_S$ ) with porosity ( $n$ ) within the cylinder of length ( $L_C$ ) are all considered, allowing for all velocities values to be expressed in terms of the measured pressure in the riser. The minor losses in the permeameter are linearized to reduce a second order ordinary differential equation and are written with the permeability of the specimen in the form of one constant for the first order term.

The effective riser length of a column of water oscillating vertically has been investigated by Zlotnik and McGuire (1998) and Zurbuchen et al. (2002) for slug tests in well risers that consider constrictions in diameter. The effective riser length of the permeameter is calculated considering the riser length plus the distance traveled by water through other sections multiplied by the reduction in velocity through those distances.

$$L_E = L_R + \left(\frac{w_C}{w_R}\right)(L_C - L_S) + \left(\frac{\tau}{n}\right)\left(\frac{w_C}{w_R}\right)L_S \quad (2.1)$$

With constant flow through the system in both directions, the velocity in the cylinder ( $w_C$ ) through the cylinder area ( $A_C$ ) is nine times less than the velocity in the riser ( $w_R$ ) through the riser area ( $A_R$ ). The effective riser length is easily calculated for the tests performed without a specimen (where  $L_S = 0$ ), while the tests performed with specimen consider the average porous area of the cylinder ( $A_P$ ) over the length traveled throughout the specimen which includes some horizontal flow. The tortuosity ( $\tau$ ) is equal to the average length of the traveled path divided by  $L_S$  (Scheidegger 1957). The speed along this path is equal to the cylinder velocity divided by the porosity, while the speed along this tortuous path is multiplied by the  $\tau$  value, which is estimated as 1.2 to start, and is discussed subsequently. The tortuosity and porosity are not directly used in the

calibration of  $k$ , but they affect the duration of the period of the oscillation so a good calibration is needed.

The conservation of momentum in the permeameter balances inertia, weight, and pressure in different proportions throughout the permeameter, with shear through the specimen. The vertical pressure gradient is first considered through the initially submerged riser length ( $L_R$ ) where the velocity is highest through the small riser area and the inertial effects are most dominant.

$$-\frac{\partial p}{\partial z} = \rho(g + \frac{dw_r}{dt}) \quad (z_0 - L_R < z < z_0 + \eta) \quad (2.2a)$$

$$p = 0 \quad (z = z_0 + \eta) \quad (2.2b)$$

where  $g$  is gravitational acceleration,  $p$  is pressure at elevation  $z$  above the datum,  $t$  is time,  $\rho$  is water density, and  $\eta$  is water level displacement above the static free surface elevation ( $z_0$ ). Equation 2.2a is integrated from the nonstatic free surface of the water level where the pressure is zero ( $z_0 + \eta$ ) down to the transducer at a depth below the static free surface ( $D_T$ ) using Equation 2.2b. The small second order term of  $\eta$  above the static free surface at  $z_0$  is neglected for simplicity.

$$p_T = \rho D_T (g + \frac{dw_r}{dt}) + \rho g \eta \quad (2.3)$$

Equation 2.3 will subsequently be combined with another equation expressing the transducer pressure ( $p_T$ ) where integration starts at the free surface of the outside water level and includes the permeability and minor losses.

The pressure outside the base of the permeameter ( $p_Z$ ) is hydrostatic at any elevation ( $z$ ).

$$p_Z = \rho g (z_0 - z) \quad (2.4)$$

This equation is considered from the free surface of the hydrostatic reservoir outside of the permeameter ( $z_0$ ) where the change in pressure is simply hydrostatic down to the base. A head loss inside of the base ( $h_B$ ) occurs at the base elevation ( $z_B$ ) at a minor loss ( $F_B$ ) where the water enters through the base area ( $A_B$ ) at velocity ( $w_B$ ).

$$h_B = F_B \frac{w_B^2}{2g} \quad (2.5)$$

The vertical pressure gradient is then considered inside the bottom of the cylinder where the velocity is slow up to the specimen. Through the specimen, the pore speed considers some horizontal flow due to the tortuosity, and is considered by multiplying the cylinder velocity ( $w_C$ ) by  $\tau$  and dividing by  $n$ . There is also a pressure change over  $L_S$  due to the specimen permeability ( $k$ ) and water kinematic viscosity ( $\nu$ ). The area of the cylinder ( $A_C$ ) is then empty again up to the riser interface.

$$-\frac{\partial p}{\partial z} = \rho(g + \frac{dw_C}{dt}) \quad (z_B < z < z_R) \quad (\text{without specimen}) \quad (2.6a)$$

$$-\frac{\partial p}{\partial z} = \rho(g + \frac{\nu}{k} w_C + \frac{\tau}{n} \frac{dw_C}{dt}) \quad (z_B < z < z_R) \quad (\text{through specimen}) \quad (2.6b)$$

where  $z_R$  is elevation of the riser bottom, and  $\nu$  is water kinematic viscosity. Equations 2.6a and 2.6b are now integrated from their limits and used to get the change in pressure from  $z_B$  to  $z_R$ . There is a head loss in the riser ( $h_R$ ) at the minor loss ( $F_R$ ) just above the contraction at  $z_R$ .

$$h_R = F_R \frac{w_R^2}{2g} \quad (2.7)$$

Equation 2.2a is now integrated from  $z_R$  up to the transducer elevation ( $z_T$ ) and combined with Equations 2.4, 2.5, and 2.7 and integrated Equation 2.6 to give a second equation of

$$p_T - p_T = \rho(L_R - D_T) \frac{dw_R}{dt} + \rho \left( (L_C - L_S) + \frac{\tau L_S}{n} \right) \frac{dw_C}{dt} + \rho \left( \frac{\nu L_S}{k} \right) w_C + \rho g(h_E + h_R) \quad (2.8)$$

Equations 2.8 and 2.3 are combined to a nonlinear second order differential equation with constants written in forms that will be simplified and linearized.

$$0 = \rho L_R \frac{dw_R}{dt} + \rho \left( (L_C - L_S) + \frac{\tau L_S}{n} \right) \frac{dw_C}{dt} + \rho \left( \frac{\nu L_S}{k} \right) w_C + \rho g(D_T + \eta + h_E + h_R) \quad (2.9a)$$

$$w_R = \frac{d\eta}{dt} \quad (2.9b)$$

$$\frac{dw_R}{dt} = \frac{d^2\eta}{dt^2} \quad (2.9c)$$

$$w_C = w_R \left( \frac{A_R}{A_C} \right) \quad (2.9d)$$

$$\frac{dw_C}{dt} = \frac{dw_R}{dt} \left( \frac{A_R}{A_C} \right) \quad (2.9e)$$

The second and third order terms of Equation 2.9a are written in terms of  $\eta$  using Equations 2.9b and 2.9c.

$$p_T = \rho \left( \frac{dw_R}{dt} \right) \left( L_R + \left( \frac{w_C}{w_R} \right) \left( (L_C - L_S) + \left( \frac{\tau L_S}{n} \right) \right) \right) + \rho \left( \frac{A_R}{A_C} \right) \left( \frac{\nu L_S}{k} w_R \right) + \rho g(D_T + \eta + h_E + h_R) \quad (2.10)$$

Equations 2.1, 2.9d, and 2.9e simplify Equation 2.10.

$$p_T = \rho L_E \left( \frac{dw_R}{dt} \right) + \rho \left( \frac{w_C}{w_R} \right) \left( \frac{\nu L_S}{k} \right) w_R + \rho g(D_T + \eta + h_B + h_R) \quad (2.11)$$

Equation 2.11 includes the head losses and  $k$  which are used to balance the position, velocity, and acceleration of the water pressure at the transducer elevation.

The head losses in the riser and base are a function of the two minor losses and the velocity squared at those locations, which both are linearized to the first order form in terms of the riser velocity and are written with the permeability as the damping oscillation frequency ( $\omega$ ). An ordinary differential equation is then used to express the water pressure in the riser as a function of time with first order constant  $\omega$  calibrated to measured data.

#### 2.4.2 Minor Losses

Minor head losses in the permeameter along with the permeability of the soil dampen the oscillations and attenuate the water level fluctuation over time. Zlotnik and McGuire (1998) considered minor losses in slug tests in the governing equation along with the friction through the soil. The minor losses are included with the permeability using a model similar to Ostendorf et al. (2005) where they calculated friction and energy losses and included them in the damping constant.

The two minor losses given in Equations 2.5 and 2.7 are summed as a total minor loss ( $F_P$ ) and rewritten in terms of the head losses and velocities.

$$F_P = F_R + F_B \quad (2.12a)$$

$$F_P = \left( h_R \frac{2g}{w_R^2} + h_B \frac{2g}{w_B^2} \right) \quad (2.12b)$$

$$w_B = \left( \frac{A_R}{A_B} \right) w_R \quad (2.12c)$$

The total minor loss is written in terms of the riser velocity using Equation 2.12.

$$F_P = \left( h_R + h_B \left( \frac{A_B}{A_R} \right)^2 \right) \frac{2g}{w_R^2} \quad (2.13)$$



### 2.4.3 Linearization

The head loss is linearized using a characteristic riser velocity ( $w_A$ ) like Ostendorf et al. (2005) used to determine the riser friction in slug tests. The displacement of one and a half periods over a characteristic time duration ( $t_c$ ) is now used to reduce the order of the differential equation.

$$w_A = \int_0^{t_c} |w_R| dt \quad (2.14)$$

Equation 2.14 is evaluated using finite difference like Ostendorf et al. (2005) did, but this is provided subsequently because it requires an estimate of  $\omega$ .

Equation 2.11 is written in terms of minor losses using Equation 2.13, with one of the velocity terms linearizing the constant of the first order term and with both sides divided by  $\rho$  and  $L_E$ .

$$0 = \frac{d^2\eta}{dt^2} + \left( \left( \frac{w_C}{w_R} \right) \left( \frac{\nu L_S}{k L_E} \right) + \frac{F_P w_A}{2 L_E} \right) \frac{d\eta}{dt} + \frac{g}{L_E} \eta \quad (2.15a)$$

$$\omega = \frac{F_P w_A}{2 L_E} \quad (L_S = 0) \quad (2.15b)$$

$$\omega = \frac{\frac{F_P w_A}{2} + \frac{\nu L_S}{k} \frac{A_R}{A_C}}{L_E} \quad (L_S > 0) \quad (2.15c)$$

The first order constants are written as a damping oscillation frequency constant ( $\omega$ ) for tests without soil (Equation 2.15b) and for tests with soil (Equation 2.15c). Equation 2.15a can now be written in the form of a damped spring equation and then be evaluated as a function of time to calibrate  $\omega$  to measured data, giving  $F_P$  for a test without soil and then  $k$  for a test with soil after  $F_P$  is calculated.

#### 2.4.4 Governing Equation and Oscillation Frequency

Equation 2.15 is written in the form of the damped spring equation with the damping oscillation frequency  $\omega$ , which is a function of friction, gravity and inertia (Van der Kamp 1976).

$$\frac{d^2\eta}{dt^2} + \omega \frac{d\eta}{dt} + \frac{g}{L_E} \eta = 0 \quad (\eta \ll L_E) \quad (2.16)$$

Equation 2.16 is now written as a closed form solution for  $\eta$  as a function of time which is similar to solutions for slug tests by Ostendorf et al. (2005).

$$\eta = \eta_0 \exp\left(-\frac{\omega t}{2}\right) \left[ \cos\left(t \sqrt{\frac{g}{L_E} - \frac{\omega^2}{4}}\right) + \frac{\sin\left(t \sqrt{\frac{g}{L_E} - \frac{\omega^2}{4}}\right)}{\sqrt{\frac{4g}{\omega^2 L_E} - 1}} \right] \quad (\eta \ll L_E) \quad (2.17)$$

where  $\eta_0$  is the initial position of the water level above the free surface at the start of the analysis. This is equal to the initial applied pressure (where  $\eta$  is negative) divided by the density and gravity, although it represents the starting pressure at the beginning of some calibrations performed on later periods of the tests to show that the flow is always laminar because  $k$  is consistent, which is discussed subsequently.

The measured pressure at  $z_T$  is about 5-10 cm below  $z_0$ , and reflects the fluctuating water level in the riser, the hydrostatic pressure, and the inertial effects due to the velocity and acceleration of the water. The order of Equation 2.3 is reduced using Equation 2.16 to consider the pressure change at the transducer elevation ( $P_T$ ), subtracting the hydrostatic pressure from each side of the equation.

$$p_T = \rho \omega w_R D_T + \rho g \frac{L_E - D_T}{L_E} \eta \quad (2.18)$$

Equations 2.17 and 2.18 combine to give the pressure change as a function of  $\eta$ ,  $\omega$ ,  $L_E$ , and time the same way that was done by Ostendorf et al. (2005).

$$P = \rho g \eta_0 \exp\left(-\frac{\omega t}{2}\right) \left[ \frac{L_E - D_T}{L_E} \cos\left(t \sqrt{\frac{g}{L_E} - \frac{\omega^2}{4}}\right) + \frac{L_E + D_T}{L_E} \frac{\sin\left(t \sqrt{\frac{g}{L_E} - \frac{\omega^2}{4}}\right)}{\sqrt{\frac{4g}{\omega^2 L_E} - 1}} \right] \quad (\eta \ll L_E) \quad (2.19)$$

Equation 2.19 calibrates  $\omega$  which leads to a calculation of  $k$  once  $F_P$  and  $w_A$  are known.

The average characteristic velocity is calculated using an estimated  $\omega$  value before the calibration of any test, and it may have to be reiterated a few times until it converges because it uses  $\omega$  implicitly. This is used exactly as Ostendorf et al. (2005) used it.

$$w_A = \frac{|\eta_0|}{3\pi} \sqrt{\frac{g}{L_E}} \left[ 1 + 2 \left( \exp\left(-\frac{\pi\omega}{2} \sqrt{\frac{L_E}{g}}\right) + \exp\left(-\pi\omega \sqrt{\frac{L_E}{g}}\right) \right) \right] \quad (2.20)$$

This equation considers the average absolute value of the velocity over the first 1.5 periods dividing the averaging interval into periods of rising and falling water levels, which is about 1.5 seconds for most tests.

#### 2.4.5 Minor Loss Calibration

A nested Fibonacci search (Beveridge and Schechter, 1970) calibrates  $\omega$  for the tests.

$$\delta = \frac{1}{N\rho g \eta_0} \sum |p_T - p_C| \quad (2.21)$$

The error ( $\delta$ ) of the calibrated pressure head is minimized where  $N$  is the number of observations of  $p_T$  in each test which were all recorded at 1,000 Hz. Figure 2.4 shows the

calibrations from the start of a test performed without a specimen considering 1.5 to 2 seconds (and 1.5 to 2 oscillations) of data. The first two seconds of data were used for most tests because the characteristic velocity reflects the average velocity over the first 1.5 seconds while the first 1.5 seconds were used for the gravel and fine gravel tests because the water level fluctuation dampens considerably more after 1.5 seconds.

The damping oscillation frequency lowers slightly with time because  $F_P$  increases as  $w_A$  decreases throughout a test, so several consecutive oscillations were calibrated to form a linear relationship between the two (0 to 2 seconds and 1 to 3 seconds are shown in Table 2.1). Equation 2.21 calibrates  $F_P$  as a function of the  $w_A$  values in the range seen in the tests with soil for most tests (0.07 to 0.02 m/s) giving  $F_P$  as a function of  $w_A$  over the two consecutive periods considered. The  $F_P$  values are calculated as a simple linear function of  $w_A$  with the calibrated  $\omega$  from Equation 2.19, the relationship and values considered are omitted because of the simplicity.

$$F_P = \frac{2\omega L_E}{w_A} \quad (L_S = 0) \quad (2.22)$$

Table 2.1: Results of tests

	Empty (first two seconds)	Empty (from 1 to 3 seconds)	V Stones	H Stones	Alpine Chips	Pond Pebbles	marbles	gravel	fine gravel
Specimen Length $L_s$ (m)	0	0	0.248	0.248	0.238	0.238	0.210	0.230	0.155
porosity $n$ (-)	1	1	0.40	0.40	0.48	0.43	0.35	0.44	0.44
$\tau$ (-)	1	1	1.54	2.22	1.78	1.52	1.09	1.64	1.48
Initial displacement $\eta_0$ (m)	0.021	0.017	0.023	0.016	0.027	0.024	0.019	0.029	0.025
$\omega$ (s <sup>-1</sup> )	0.62	0.51	0.84	0.88	1.20	0.89	1.24	4.65	4.77
$F_p$ (-)	3.27	3.54	4.49	5.56	4.26	4.38	4.35	6.32	6.41
$k$ (m <sup>2</sup> )	-	-	3.6E-07	1.8E-07	1.7E-07	3.4E-07	1.2E-07	2.1E-08	1.5E-08
$K$ (m/s)	-	-	3.5	1.7	1.6	3.3	1.14	0.20	0.15
$K_{10}$ (m/s)	-	-	2.7	1.3	1.3	2.6	0.87	0.15	0.11
model error $\delta$ (%)	4.8	2.7	4.4	6.5	5.5	6.7	5.2	4.3	6.4
char. riser velocity $w_A$ (m/s)	0.074	0.056	0.060	0.038	0.065	0.063	0.046	0.031	0.030
$d_{50}$ (m)	-	-	0.035	0.045	0.023	0.029	0.015	0.008	0.005
Reynolds number	-	-	230	186	163	201	76	28	16
$D_T$	0.085	0.085	0.106	0.106	0.081	0.084	0.082	0.085	0.085

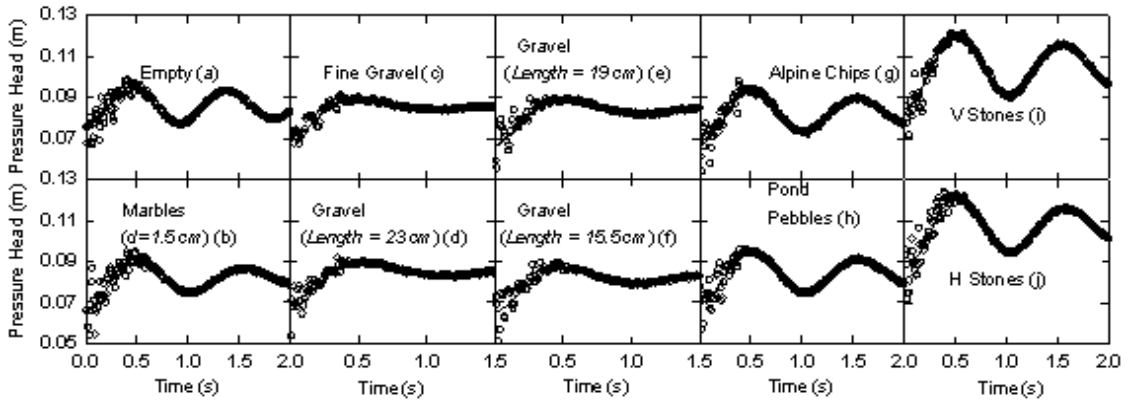


Figure 2.4: Pressure fluctuations (circles) and calibrations (lines) from the static value ( $D_T$ )

## 2.4.6 Hydraulic Conductivity Calibration

Equation 2.19 is used with Equation 2.20 (just as described before) to calibrate  $\omega$  to the measured pressures using the appropriate  $F_p$  value for a test performed with soil. The permeability of the specimen is calculated using Equation 2.19 with  $w_A$  and the calibrated  $F_p$  value.

$$k = \frac{\left(\frac{D_R}{D_C}\right)^2 v L_S}{L_E \omega - \frac{F_p |w_A|}{2}} \quad (2.22)$$

The hydraulic conductivity at the temperature measured (20°C) is shown as  $K$  but it is also calculated at 10°C ( $K_{10}$ ) which represents the insitu temperature using the temperature dependent  $\nu$ .

$$K = \frac{kg}{\nu} \quad (2.23)$$

## 2.5 Results

Table 2.1 gives the results of two calibrations of the empty chamber and one calibration for each of the soils considered. The calibration curves have excellent fits; the average absolute difference between measured and predicted pressure head over the duration considered being on the order of 1 mm, or 5% of the initial displacement. The amplitudes of the more permeable specimens (such as Figure 2.4g through 2.4j) have less decay, as shown by the lower  $\omega$  values because of the higher  $K$  values. The three calibrations for the same gravel but with different specimen lengths have different amplitudes (Figure 2.4d, 2.4e, and 2.4f) as a result of the different  $\omega$  values due to varying specimen lengths, while Table 2.2 shows that the relative standard deviation of computed  $K$  values for all three specimen lengths is only 5%.

The duration of the period of the oscillations varies proportionally to  $\sqrt{L_E}$  and is about 1 second for tests with a specimen and 0.9 seconds without a specimen. The accuracy of  $L_E$  (within 1 cm) is very important in obtaining a satisfactory match of theoretical and measured curves and is found by iterating  $\tau$  values in Equation (2.1). Figures 2.4d and 2.4e show that there is a notable difference in the period of the H Stones with larger  $\tau$  values (2.22) than the V stones (1.54) as expected, because the path traveled against the larger diameter of an oval is longer than the smaller diameter. Although the

porosity and length of the two samples are the same, the period of the oscillation of the H Stones specimen is noticeably longer because  $L_E$  is larger. The alpine chips have slightly higher  $\tau$  values (1.78) than the Pond Pebbles (1.52), possibly because they are more angular. The marbles have the smallest  $\tau$  values (1.06), likely because of their perfect sphericity. The tortuosity is known to affect the hydraulic conductivity of soil but is difficult to estimate. Matyka et al. (2008) used a microscopic model to find the tortuosity of porous media to be about 1.2 to 1.8 within the porosity values found in this study, with higher tortuosity values for lower porosities and longer specimens.

The hydraulic conductivity of the marbles calculated using the Kozeny-Carman equation at 10°C is 0.84 m/s, within 5% of the calibrated values from the two tests performed; just like Ferreira et al. (2010) were within 1% for pebbles with diameter of 1 cm. The uniform pebbles tested by Ferreira et al. (2010) were smaller and had a higher porosity (0.40) than the marbles tested in this study, but the results of all of their tests performed within the Darcian regime also matched the Kozeny-Carman model just like the results of this study did. The Kozeny-Carman model is the most commonly used grain size model used because it considers the porosity and surface area of the soil tested. Its accuracy is slightly reduced when soils considered have a large distribution of grains, or if the gradation is not well known. Therefore, these two test methods yield results that are more precise than any found in the literature for uniform spheres.

The  $K$  values calculated for the three gravel specimens are about twice as high as constant head tests performed, which is likely due to difficulty measuring and keeping the Mariott bubble tube used for these tests to maintain a 0.5 to 1 cm of head to the specimen, which was done to keep the Reynolds number the same as that for the tests

performed in the new permeameter. Furthermore, the bubble typically formed a large meniscus when small heads were applied, and was released from the bubble tube relatively slowly which likely affects the applied head. Turbulent flow was likely not present during these tests because the  $K$  values were consistent but frictional losses in the system could explain why the  $K$  values were lower; all friction in these tests was attributed to the soil.

The hydraulic conductivity values of several specimens were additionally calibrated considering one or two later periods after the first two (i.e. from 1 to 3 seconds and 2 to 4 seconds) until the response was too dampened. These calibrations yielded consistent  $K$  values, assuring that the flow was laminar at the beginning of the test. If it were not laminar, then the beginning values calibrated with the highest velocities would have yielded erroneously low  $K$  values. The relative standard deviation of the calibrated  $K$  values was a maximum of 10% for specimens less permeable than 1 m/s to 24% for the most permeable specimens (Table 2.2). The higher variability in the more permeable specimens is a result of the smaller influence that the high permeability has on the damping of the oscillations because head losses of those tests are larger than the friction from the specimen permeability and there is no trend in variability of  $K$  as the oscillations decay. The Reynolds numbers were calculated using  $d_{50}$  (the grain diameter with 50% finer), kinematic viscosity and the average vertical velocity through the cylinder. The  $d_{50}$  values of the stones reflect the approximate diameter facing the direction of flow (0.035 and 0.045 m). Table 2.3 compares the Reynolds number,  $d_{50}$ , and  $K$  for several sources listed as well as results of this study.



The hydraulic conductivity values are compared with the ballast tested by Tennakoon et al (2012) who reported  $K$  values of 0.3 m/s where they were tested in a constant head permeameter where the hydraulic gradient was about one. They did not verify that the flow was laminar, only stating that using a gradient less than four would result in nonlaminar flow but a calculation of their Reynolds number shows that it was over 10,000. A comparison of the grain size curve of their ballast to the pond pebbles in this study suggests that this ballast would be about 3 m/s using the analysis in this study, ten times higher. Ferreira et al. (2010) experimentally determined that a gradient of 0.0015 or lower was required for laminar flow on pebbles with a diameter of 1 cm, so the gradient was clearly too high, which explains the lower hydraulic conductivity value. The other literature reporting hydraulic conductivities this high were found in NAVFAC (1986), which were cited by Trani and Indraratna (2009) who modified the Kozeny-Carman equation using the grain size distribution and measured hydraulic conductivity values from several sources. The most permeable of these data are shown in Figure 2.3 with results from this study. Because the grain size distribution is different for every sample besides the uniform pebbles and marbles, a qualitative assessment of Figure 2.3 is the best way to compare the hydraulic conductivity values in this study to these results. These tests are all about three to five times less permeable than the values found in this study of comparable soils. This could suggest that the flow was not laminar for the other tests performed. It could also be an incorrect temperature or porosity value which was likely not available and estimated, but the nonlaminar flow is more likely the explanation because the values are consistently lower much like the constant head tests performed on the gravel. Also, their sample of uniform with a diameter of 1 cm has a hydraulic

conductivity value that is three times less than the value found by Ferreira et al. (2010), who had  $K$  values that matched the Kozeny-Carman model this study. The Kozeny-Carman model can be used with the results of this study to evaluate the differences the grain shape has on  $K$  as well as the parameters tested e.g. (grain size and distribution,  $n$ , and  $\tau$ ).

Table 2.2: Statistics of calibrations

	V Stones	H Stones	Pond pebbles	Alpine chips	marbles	gravel
number of tests considered	3	3	2	2	2	3
number of periods considered	9	7	6	6	6	3
average $K$ (m/s)	3.0	1.7	3.6	1.7	1.1	0.20
standard deviation of $K$ (m/s)	0.72	0.39	0.75	0.19	0.11	0.01
relative standard deviation of $K$ (m/s)	0.24	0.23	0.21	0.11	0.10	0.05

Table 2.3: Reynolds number comparison

	$K$ (m/s)	Reynolds Number (-)	$d_{10}$ (m)	$d_{50}$ (m)	Specific discharge (m/s)
<i>Plain + Morrison</i>	0.010	100		1.3E-03	
<i>Ferriera OFG</i>	0.040	10	3.0E-03	7.0E-03	6.0E-04
<i>Ferriera pebbles</i>	1.0	25	1.0E-02	1.0E-02	2.0E-03
<i>Cedergren Gravel 1</i>	0.40	31	1.5E-02	2.0E-02	1.5E-03
<i>Cedergren Gravel 2</i>	1.6	151	2.8E-02	3.3E-02	4.6E-03
Fine gravel	0.15	16	3.0E-03	5.0E-03	3.3E-03
Gravel	0.20	28	6.0E-03	8.3E-03	3.4E-03
Marbles	1.1	76	1.5E-02	1.5E-02	5.1E-03
Alpine Chips	1.6	163	1.6E-02	2.3E-02	7.2E-03
Pond Pebbles	3.3	201	2.1E-02	2.9E-02	7.0E-03

## 2.6 Conclusions

A permeameter has been designed and constructed to determine the hydraulic conductivity of gravels ranging from 0.1 to 1 m/s. The tests are commenced by applying 200 to 300 Pa (2 to 3 cm of water level displacement) of air pressure to a water column in a small-diameter riser above a saturated cylinder with gravel specimen. The pressure is

rapidly released allowing water to flow through the base of the cylinder and the specimen while the water column level oscillates about the static value in an underdamped response. Fluctuations of the water level in the riser are measured and recorded at a frequency of 100 Hz.

The underdamped responses oscillate about the static value at frequency at about 1 Hz and are sensitive to the hydraulic conductivity of all tested materials. The inertia and friction in the permeameter affecting the response are calculated and verified by the small model error while the closed form analytical model developed here calibrates the permeability using a closed form model. Using this model that considers the permeameter geometry, the permeameter effects can be estimated separately by calibrating the model results with data from tests performed without a specimen. The hydraulic conductivity is then calibrated by accounting for the head losses of the permeameter for each test with a specimen. The average error in predicting the head values is 1.3 mm, or about 5% of the initial displacement for all tests. The permeability values calibrated for three gravel tests with different specimen lengths are within 5% of the median value, which is very precise because the measurements of specimen length cannot be performed with much better precision. The permeability value of the marbles calculated using the Kozeny-Carman equation is within 5% of the calibrated value, which is the most accurate grain size model to use since the specific surface is known.

## CHAPTER 3

### USING THE KOZENY-CARMAN EQUATION TO PREDICT THE PERMEABILITY OF GRAVELS

The permeability and tortuosity of gravel specimens ranging from ( $2 \times 10^{-8} \text{ m}^2$  to  $2 \times 10^{-7} \text{ m}^2$ ) were calibrated to measured pressure readings using the model presented by Judge et al. (*in press*) which utilizes a modified permeameter that induces oscillatory responses. The porosity and grain size distribution of the specimens were measured while the surface area was determined by evaluating the shape and angularity of subrounded and angular soils each arranged to the same six different gradations. The Kozeny-Carman equation was used with these parameters including the tortuosity as suggested by Scheidegger (1957) and paired with the measured permeability values that are more precise and accurate than most data in the literature. The Kozeny-Carman equation was used to empirically determine the packing factor which was observed to increase by a factor of the tortuosity cubed for these tests as well as select results from Judge et al. (*in press*) that have different tortuosity values. The permeability values of the 12 specimens were predicted to be within an average factor of 1.2 of the measured values and all within a factor of 1.4.

#### 3.1 Introduction and background

Gravels are extensively used for roadway construction, drainage curtains, and railroad ballast. In some projects the gravel must be able to provide a minimum and high enough rate of drainage so engineers and contractors often need to measure it directly to prove that their source material or an existing material has an acceptable permeability. Chapuis and Aubertin (2003) noted that the accuracy of laboratory permeability tests

(e.g., ASTM 2012) for coarse materials is often questionable because the measured values from three replicate tests may vary significantly. This lack of precision partially depends on test equipment and procedures in addition to the natural variability of the tested material. As an alternative to making direct measurements, empirical correlations with grain size are often used to estimate the permeability since a grain size distribution test is quick and easy to perform, but such correlations are typically considered to only give an order of magnitude estimate. However, if several reliable soil properties are considered, the accuracy of these correlations can be enhanced. This is demonstrated and verified in this paper for two coarse gravels because the predicted permeability values of the presented soils are very close to the measured results tested using the permeameter and theory described by Judge et al. (*in press*).

Judge et al. (*in press*) calibrated the permeability and tortuosity of gravels and materials using a model that considers a modified permeameter. It was used by applying an instantaneous change in head to a smaller diameter riser above the specimen, inducing an oscillatory response which decays as a function of the permeability just like in an underdamped slug test (Ostendorf et al. 2005). Included in their tests were perfectly spherical marbles and oblong (and anisotropic) stones that were less spherical than the other soils, and tested in two orientations yielding different tortuosity values. The permeability of the marbles calibrated by Judge et al. (*in press*) was equal to Kozeny-Carman model whether the tortuosity was considered or not because the tortuosity was found to be small and the surface area was known. The marbles were used for comparison and a basis for the packing factor because spheres were empirically investigated by Carman (1956). The anisotropic stones tested with the flow in the

direction of the long axis of the stones and against it were also evaluated here because the only different soil parameter is the tortuosity which has a clear effect on the permeability. These findings led to the motive to use this equation with results from natural soils of complex shapes and tortuosity values tested by this device, which additionally required a means of quantifying the surface area of the soil tested.

The purpose of this manuscript is to use the measured permeability, grain size distribution, shape, porosity, and tortuosity values from the tests performed on two soils evaluated using the model of Judge et al. (*in press*) to assess the accuracy of the Kozeny-Carman equation which has a packing factor that can be empirically evaluated. The effects of the shape factor, porosity, and grain diameter and grain size distribution on the permeability can be qualitatively compared by considering the tests performed on two soils of different angularity arranged to different grain size distributions. Figure 3.1 shows a photograph of these two soils collected from a gravel pit and their gradations of well (log normally distributed), uniform (with soil from two adjacent sieves), and skew (in between the other two, commonly found).

The Kozeny-Carman equation is the most accurate grain size model that can currently be used for estimating the permeability ( $k$ ) because it considers the porosity ( $n$ ) and surface area of the soil tested.

$$k = \frac{n^3}{(1-n)^2} \frac{d_{eff}^2}{C_{SH}^2 C_{PK}} \quad (3.1)$$

The packing factor ( $C_{PK}$ ) was empirically determined by Carman (1956) to be equal to 5 for uniform spheres, and this value has been used by most researchers since then. The permeability is shown as  $k$  in ( $m^2$ ), and  $d_{eff}$  is the effective diameter (usually taken as the average or a lower bound value). The shape factor  $C_{SH}$  varies from 6 (for round) to 8 (for

angular and surrounded soils), coming from Equation 3.2 where  $SA$  is the surface area and  $V_S$  is the volume of solids.

$$C_{SH} = \frac{SA}{V_S} d_{eff} \quad (3.2)$$

The shape factor reflects the effects of the surface area for a given volume of soil (with an effective diameter), as described by Fair and Hatch (1933).

Chapuis and Aubertin (2003) evaluated the Kozeny-Carman equation by evaluating literature results of specimens with a variety of grain size distributions and void ratios that had a known grain size distribution and a measured  $k$  value. They considered the distribution of grain sizes and found the Kozeny-Carman results to be within a factor of three of the measured results for soils where  $k$  ranges over orders of magnitude, some of which had  $k$  values higher than  $1 \times 10^{-8} \text{ m}^2$ . The observed discrepancies were attributed to practical reasons such as inaccurate surface area values, unsteady flow, unsaturated specimens, etc. Theoretical reasons were said to also include anisotropy, motionless water in the specimens, or bridging within the specimen and roundness coefficients. The accuracy and precision of the measured  $k$  and grain size distribution values of the tests they considered were unknown, and are very likely less than satisfactory in some cases, especially for soils with high  $k$ . The predicted permeability was within a factor of three times more or less than the measured  $k$  and noticeably higher than measured for most gravels. If more accurate soil properties were used then the Kozeny-Carman equation would predict values with better accuracy.

Ferreira et al. (2010) performed constant head tests on marbles and open-framework gravel using a megapermeameter. These tests yielded  $k$  values that matched those calculated using the Kozeny-Carman equation on marbles, which verified that their

procedure of determining  $k$  was valid, just as Judge et al. (*in press*) did. Ferreira et al. (2010) also tested one specimen of open-framework gravel and used the Kozeny-Carman equation to solve for  $k$  but did not use it to validate their method for that specimen because the shape factor was unknown. Having reliable soil parameters such as the porosity, tortuosity, and effective diameter determined by a sieve analysis for a tested soil and pairing them up with more accurate  $k$  values allowed for further assessment of the Kozeny-Carman equation in this study. The tortuosity squared was suggested to be considered in the denominator of Equation 3.1 by Scheidegger (1957), Costa (2006) and a few others, though it has been rarely evaluated and used. Furthermore, if the roundness and angularity were estimated by a method of determining the shape factor, this equation would be more accurate (Carman 1956).

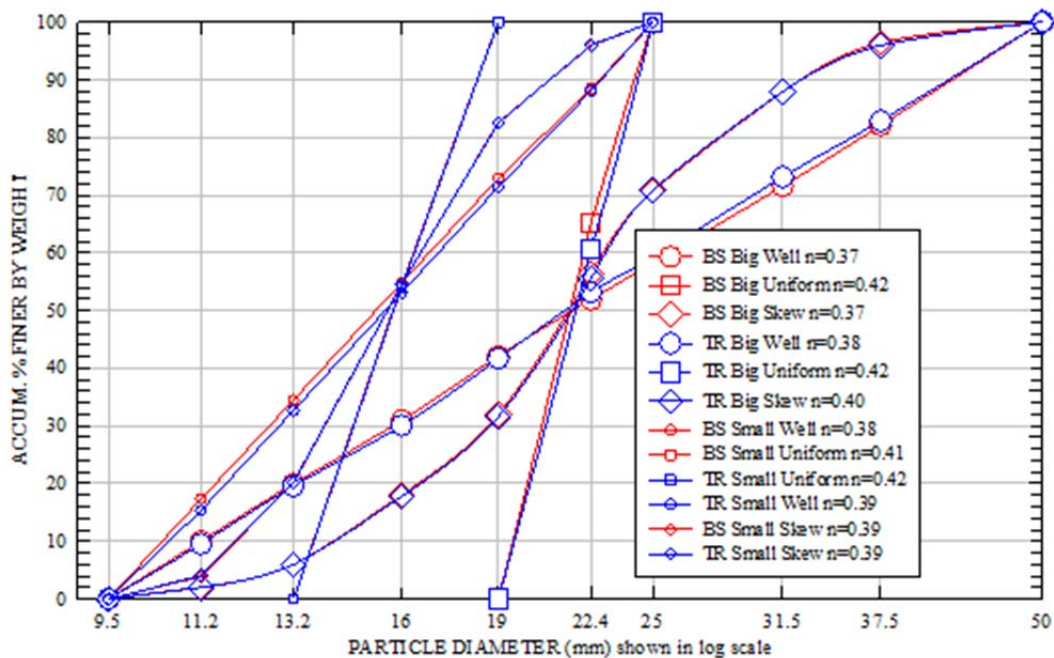


Figure 3.1: Grain Size Distribution of the Brown Stone (BS) and Tap Rock (TR). Tap Rock is shown in the left of the photograph and Brown Stone is shown in the right.



## 3.2 Tests performed and procedures

The grain size distribution and porosity of gravel specimens are typically available while the other factors are rarely known or used. The packing factor is usually set at 5 while the shape factor is usually given a value from 6 to 8. Judge et al. (*in press*) performed laboratory permeability tests on gravels and calibrated  $k$  and  $\tau$  with precision within 10% of replicate tests for specimens as permeable as  $1 \times 10^{-8} \text{ m}^2$ . Three tests were performed on each specimen; the results of two of these tests were averaged and used. The shape and angularity were quantified independently in this paper using measurements and theory. The following sections describe the various soil and specimen properties considered and how they were determined for use in Kozeny-Carman equation. The shape factor is quantified, the tortuosity is used, and the packing factor is considered using a new equation.

### 3.2.1 Porosity and tortuosity

The tests performed had a specimen length ( $L_S$ ) of 0.23 meters. The porosity was determined by measuring the mass of the test specimen and dividing by the volume to get the dry density. This value was divided by the density of solids ( $\rho_S$ ) which was assumed to be  $2.7 \text{ g/cm}^3$  and subtracted from one. The volume of solids ( $V_S$ ) of each specimen was calculated by dividing the total mass ( $m_T$ ) by the density of solids ( $\rho_S$ ) using Equation 3.3. This is also done for the volume of individual grains by dividing the mass of the grain ( $m_G$ ) by  $\rho_S$  using Equation 3.4.

$$V_S = m_T / \rho_S \quad (3.3)$$

$$V_G = m_G / \rho_S \quad (3.4)$$

The tortuosity ( $\tau$ ) of the specimens was determined by calibrating the measured pressure of a test to the model of Judge et al. (*in press*) simultaneously with  $k$ . The porosity causes higher pore velocity which increases the inertial effect and consequently the time period ( $t_C$ ) of each fluctuation seen in Figure 3.2 (one second). The permeability of the soil causes a decay of the oscillation, dampening the amplitudes  $h(t)$  which peak (from the static value  $h_0$ ) when  $t_C$  is a multiple of 0.5. The pressure difference through the specimen was integrated, considering the changes in velocity through the porosity along the calibrated average path ( $\lambda$ ) of the water through the specimen length (Figure 3.3). The tortuosity was then calculated with the calibrated  $\lambda$  as it is defined in Equation 3.5.

$$\tau = \lambda/L_S \quad (3.5)$$

The only other method to determine  $\tau$  found in the literature was to estimate it using tritium breakthrough curves, results of a microscopic model of overlapping spheres by Matyka et al. (2008), or to use electrical methods as suggested by Scheidegger (1957). The tortuosity ranged from 1.1 to 1.4 for the two gravels tested in this study, which is within the theoretical range of 1.1 to 1.2 predicted for coarse soils by Hamamoto et al. (2012). Two specimens of oblong stones tested by Judge et al. (*in press*) were arranged where  $\tau$  was calibrated to be 2.2 (measured  $k = 3.2 \times 10^{-7} \text{ m}^2$ ) when the grains were aligned with the long axis against the flow and 1.5 (measured  $k = 1.8 \times 10^{-7} \text{ m}^2$ ) in the direction of the flow. This shows that tortuosity affects  $k$  because anisotropy was the only difference between the two. It should also be noted that  $\tau$  was not directly used to measure  $k$ , but rather the response of the horizontally aligned specimen decayed more rapidly (due to lower  $k$ ) and had a slightly longer period (yielding a higher  $\tau$ ). These

resulted in different calibrated values for  $k$  and  $\tau$  before consideration of the Kozeny-Carman equation with all other parameters equal. This further verifies that  $\tau$  needs to be considered in the Kozeny-Carman equation at least for highly permeable soils where  $\tau$  is significant (greater than 1.1).

Matyka et al. (2008) noted that  $k$  decreases linearly with  $\tau^2$  using the analogy of flow through curved pipes divided by the straight distance. Scheidegger (1957) also noted this and included  $\tau^2$  in the denominator of permeability equations he proposed in the form of the Kozeny-Carman equation. Costa (2006) noted that the permeability decreases linearly with  $\tau^2$  because the packing factor increases as a function of tortuosity. The model presented by Judge et al. (*in press*) gives  $\tau$  for soils where  $k$  is greater than  $k = 1.8 \times 10^{-8} \text{ m}^2$  because the inertial effects are seen but not less, so testing gravels of high permeability is an advantage here.

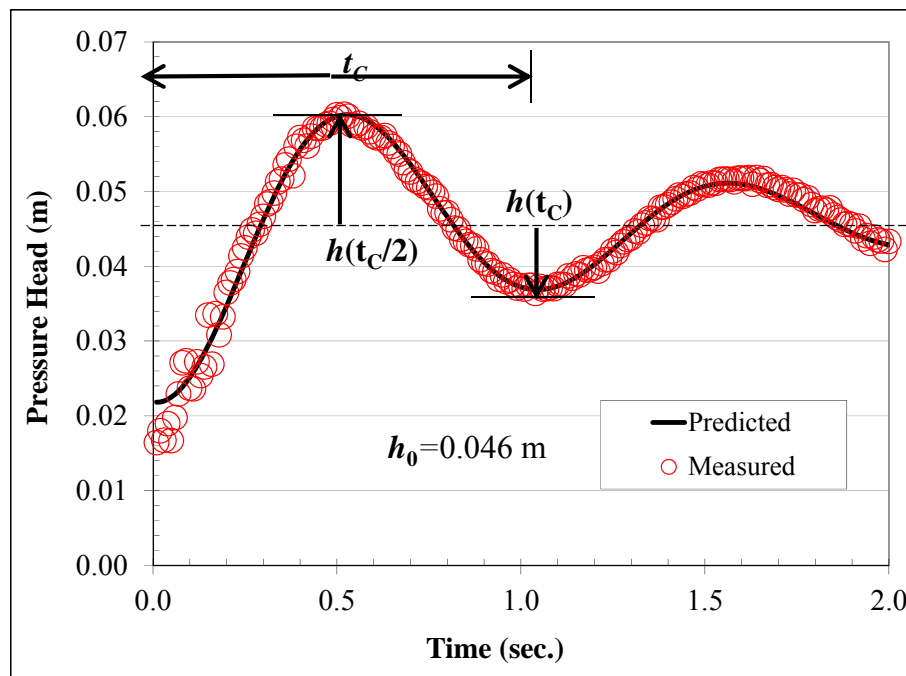


Figure 3.2: Measured and calibrated pressure head for the Brown Stone small well graded specimen

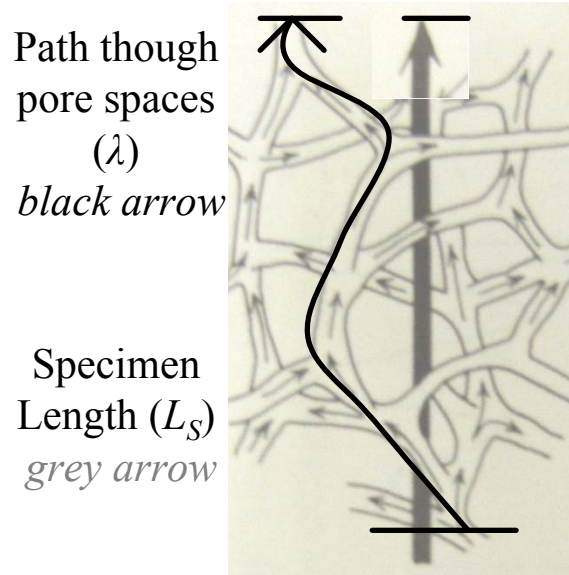


Figure 3.3: Tortuosity through a specimen of soil (from Fair and Hatch (1933))

### 3.2.2 Grain size distribution

The grain size distribution was determined using a nest of nine sieves in order to capture more detailed information on the grain size distribution as compared to the common practice of using fewer sieves with larger gaps between consecutive sieve sizes. The sieves used range from 9.5 to 50 mm opening, as shown in Figure 3.1. Carrier (2003) noted that the effective grain diameter is typically a logarithmic function between adjacent sieves and the diameter is best represented by Equation 3.6 where  $d_s$  is the smaller sieve diameter and  $d_l$  is the larger sieve diameter.

$$d_{eff} = d_s^{0.6} d_l^{0.4} \quad (3.6)$$

This diameter represents the theoretical diameter of the smaller two axes of a gravel particle passing through a sieve while the third axis is usually the longest one. It is typical to calculate the surface area of a grain with this effective diameter (assuming a sphere) and then comparing this value to the average diameter of the soil tested. This

effective diameter of a sphere is commonly used with the surface area to back calculate the shape factor of the two soils to compare to the values given for the visual examples provided by Fair and Hatch (1933). An ellipsoid was considered for the soil grains in this study for better accuracy.

The ellipsoid shape was first measured, and then the angularity of the surface was determined by considering the edge of the grains to the perimeter in three projected sections of the grain. The surface area of a grain is affected by the shape and angularity of the soil, which was separately quantified in order to calculate the surface area to volume of solids ratio of ellipsoid shaped grains with accuracy. The large particles were easier to evaluate than the smaller ones, which was another advantage of using this method with coarse gravel.

### **3.2.3 Soil grain shape**

A uniform sphere has a shape factor of 6 defined in Equation 3.2. A sphere with a surface area that is rougher by an angular factor would have a shape factor equal to 6 times that angular factor (Figure 3.4) which is typically assumed a value of 6 to 8 based on the examples provided by Fair and Hatch (1933) but is sometimes measured. Since coarse grains commonly resemble ellipsoids rather than spheres, the ellipsoid shape is considered in this paper. A smooth grain with the shape of an ellipsoid can have a shape factor as high as 8 or so while a rough one can be even higher. The shape is first considered, and then the angularity is considered because the surface area of an ellipsoid cannot be calculated with a unique shape factor like a sphere can be. A surface area to volume ratio is needed for each of the nine grain size groups of  $d_{eff}$  to calculate an average value for  $C_{SH}$ .

The shape of the ellipse of a given gravel particle was first determined by measuring the three principal axes. The three measured axes ( $a_m$ ,  $b_m$ , and  $c_m$ ) of three grains randomly selected from each of the nine size groups of two soils considered were measured using a micrometer to determine the shape of the grains as illustrated in Figure 3.4. The axes measured are often larger or smaller than the axes that would calculate an ellipsoid of an equivalent volume because of the irregular shape of the grains.

The volume factor ( $C_V$ ) was calculated as the volume of a grain divided by the volume of an ellipsoid calculated using the measured axes as

$$C_V = V_G / \left( \frac{\pi}{6} a_m b_m c_m \right) \quad (3.7)$$

The volume factor was used to adjust the measured axes to adjusted axes that retain the measured shape but calculate the actual volume using Equations 8 through 10.

$$a = a_m C_V^{(1/3)} \quad (3.8)$$

$$b = b_m C_V^{(1/3)} \quad (3.9)$$

$$c = c_m C_V^{(1/3)} \quad (3.10)$$

This step was necessary because the overall surface area of the grain differs from that of an ellipsoid formed from measured axes by different proportions than it does from the axes forming the same volume. This extra step provides better accuracy and requires several steps.

Figure 3.4 shows that there are three projected sections of the grains considered that are used to determine the perimeter of the edge of each projected section, which were used to calculate the surface area of an ellipsoid of the same volume as the grain. These edges were compared by measuring the perimeter edge of the projected sections. The

average ratio of the perimeter of the edge of the projected section to the perimeter of the ellipse of that projected section is the same ratio of the surface area of the grain to the ellipsoid. This factor was then used to determine the average surface area to volume ratio of grain.

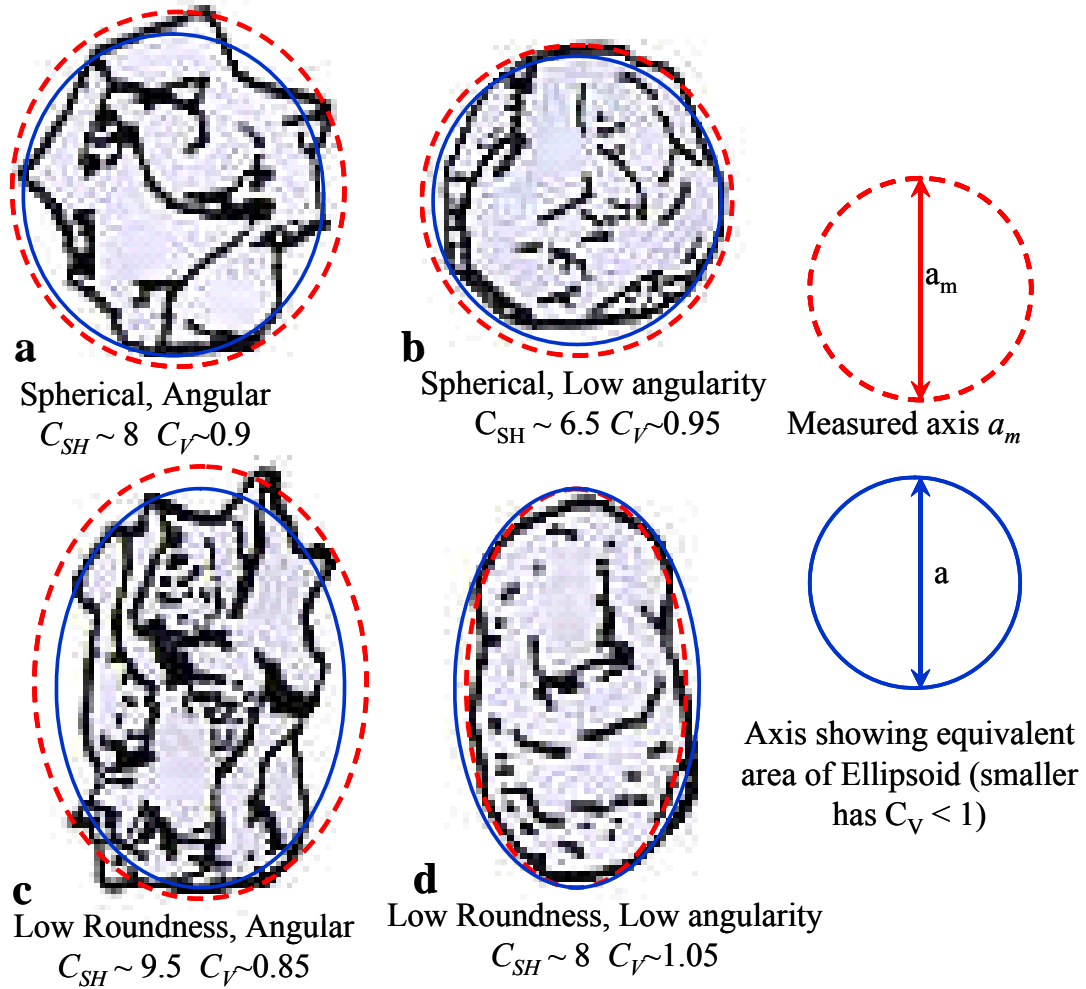


Figure 3.4: The effects of angularity and shape on the shape factor ( $C_{SH}$ ) and a comparison of the measured axes vs. the equivalent axes and their effect on the volume factor ( $C_V$ ). Note that: The volume and shape of 'a' equals 'b' and the volume and shape of 'c' equals 'd'.

### 3.2.4 Calculation of grain angularity and surface area using perimeter measurements

Photographs of each projected section were taken and imported into AutoCAD. They were scaled by including a marble with a known diameter at the same distance from the camera as the grains considered. The grain edges were then traced, providing the perimeter of each. The perimeter ( $P$ ) of each projected section differs from the perimeter of an ellipse with the same area ( $P_e$ ) because the edge is rough as shown in Figure 3.4. Equation 3.11 is used for the perimeter of an ellipse.

$$P_e = \pi \left[ 3 \frac{a+b}{2} - \left( 3 \frac{a}{2} + \frac{b}{2} \right) \left( 3 \frac{b}{2} + \frac{a}{2} \right)^{0.5} \right] \quad (3.11)$$

The surface area factor ( $C_{SA}$ ) is calculated using the three projected sections to determine how much greater the perimeter is for each section than an ellipse of similar shape and equivalent area.

$$C_{SA} = P / P_e \quad (3.12)$$

The shape of the grain is retained using the adjusted axes (a, b, c) and the volume of the ellipsoid is equal to the volume determined from weight using Equation 3.4. The angularity is considered by dividing the perimeter of the grain by the perimeter of the ellipse.

Adjusting the measured axes to represent the same volume was required because errors in the lengths of the axes usually result in erroneously large values of the surface area of the ellipsoid by proportions that vary with every shape (Figure 3.4). The surface area of an ellipsoid ( $SA_e$ ) with the same volume and shape of the grain considered is first calculated using Knud Thomsen's formula where  $p$  is a mathematical factor equal to 1.6075.



$$SA_e = 4\pi \left( \left( \left( \frac{a}{2} \right)^p \left( \frac{b}{2} \right)^p + \left( \frac{a}{2} \right)^p \left( \frac{c}{2} \right)^p + \left( \frac{b}{2} \right)^p \left( \frac{c}{2} \right)^p \right) / 3 \right)^{p-1} \quad (3.13)$$

There was no trend in  $C_{SA}$  with grain size or plane so the values of the larger four grains were all averaged (Figure 3.5). The surface area of each grain ( $SA_G$ ) considered was divided by the mass of the grain. Although the grains are not spherical, they all have a similar shape so the surface area only varies with volume (or  $d_{eff}$ ) for a given shape. The data followed this trend from the smallest to the largest as expected, with some outliers due to grains that differ broadly or were tough to measure accurately such as the smallest ones. The largest grains provided the most reliable data, so a curve was fit through those data to represent all the grain sizes. The average shape factor obtained Equation 3.16 using the data from Figure 3.5 is used for each of the nine groups.

$$SA_G = SA / g \quad (3.14)$$

$$SA = \sum_d (SA_G) m_G \quad (3.15)$$

$$C_{SH} = SA_G d_{eff} \rho_s \quad (3.16)$$

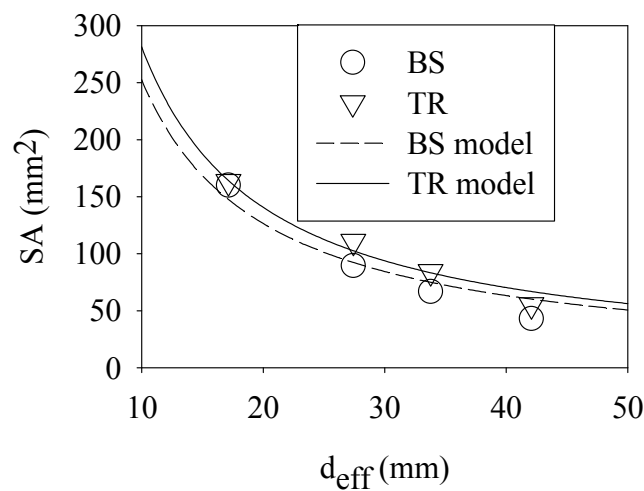


Figure 3.5: Surface area vs. effective diameter for the grain sizes considered

### 3.2.5 Packing factor

A dimensionless packing factor of 5 was empirically found to work for glass spheres by Carman (1956) who noted that it was theoretically equal to 2 for straight tubes, but increases as the tubes are tortuous and the channels have a higher ratio of cross sectional perimeter squared to area. The tortuosity squared is sometimes suggested in the denominator of the Kozeny Carman equation but it has rarely been used because  $\tau$  values are rarely obtained. Here, Equation 3.1 is used as is with the measured tortuosity considered in the packing factor.

The tortuosity considered is theoretically squared for water flow through inclined pipes (Costa 2006), and it also is for air flow through dry soil (Moldrup et al. 2004) who found the exponent to become higher than two when water became present. This same phenomenon is believed to occur for water flow through soils with complex tortuosities due to tortuous paths that have more variability within the specimen, even with the same average value. This suggests that the equation should have tortuosity to a power higher than two in the denominator. The packing factor is calculated with this tortuosity to a power of three which was observed to predict permeability values close to those measured as shown in Table 3.1 where the values of the exponent ( $\eta$ ) are 3.3 on average with only a slight trend of an increase in diameter.

$$C_{PK} = 5\tau^\eta \tag{3.17}$$

The packing factor is still very close to 5 for the marbles whether or not  $\tau^\eta$  is considered because it is so close to one.

Table 3.1: Permeability predictions and soil parameters using the Kozeny Carman equation with the packing factor as described in Equation 3.17 with  $\eta = 3$ .

	$d_{eff}$ (mm)	$n$ (-)	$(V_{Sv}/SA)$ (mm <sup>-1</sup> )	$\tau$ (-)	$\eta$	$k_m$ (m <sup>2</sup> )	$k_p$ (m <sup>2</sup> )	$\delta$ ( $k_p/k_m$ )
BS Big well graded	24	0.367	2.81	1.29	3.8	7.4E-08	9.1E-08	1.23
BS Big skew graded	22	0.374	2.95	1.14	4.6	9.6E-08	1.3E-07	1.35
BS Big uniform	21	0.416	3.12	1.27	4.3	1.5E-07	2.0E-07	1.36
BS Small well graded	16	0.375	2.13	1.39	2.3	6.3E-08	5.1E-08	0.81
BS Small skew graded	16	0.389	2.21	1.26	3.1	7.5E-08	7.7E-08	1.02
BS Small uniform	16	0.405	2.26	1.28	3.5	8.0E-08	9.0E-08	1.13
TR Big well graded	24	0.380	2.52	1.21	3.4	9.5E-08	1.0E-07	1.08
TR Big skew graded	22	0.398	2.66	1.14	4.8	1.3E-07	1.6E-07	1.27
TR Big uniform	22	0.420	2.82	1.20	4.4	1.6E-07	2.0E-07	1.28
TR Small well graded	16	0.392	1.94	1.24	1.6	8.8E-08	6.5E-08	0.74
TR Small skew graded	16	0.399	1.99	1.28	2.4	7.8E-08	6.7E-08	0.86
TR Small uniform	16	0.416	2.03	1.13	3.8	1.1E-07	1.2E-07	1.10
<i>Judge et al. (2013)</i>								
<i>marbles</i>	15	0.350	2.50	1.06	1.7	1.1E-07	1.2E-07	1.10
<i>V Stones</i>	15	0.410	5.56	1.54	3.1	3.2E-07	3.4E-07	1.06
<i>H Stones</i>	15	0.410	5.56	2.22	2.4	1.8E-07	1.1E-07	0.63
Average:								0.89
Standard Deviation:								0.22
Relative Standard Deviation:								0.25
BS $C_{SH} =$		6.8						
TR $C_{SH} =$		7.6						

### 3.3 Results

Equation 3.1 was used to predict the permeability of the twelve specimens with approximations of  $C_{SH}$  taken from Fair and Hatch (1933) as noted in Table 3.1. The permeability is predicted more than twice as high as the measured with a packing factor of five. These findings along with the anisotropic stones tested by Judge et al. (*in press*) were motives to consider the tortuosity which properly lowers the predicted  $k$ . The surface area method described in this paper was found to yield  $C_{SH}$  values that are very close to the approximations given by Fair and Hatch (1933) which suggest that it is a valuable way to determine these factors. The consideration of the tortuosity cubed in the packing factor using Equation 3.17 provides  $k$  values lower than the original

overpredictions within an absolute factor of 1.4 of the measured value, an average of 1.2, and relative standard deviation of 0.25.

$$\delta = \frac{k_p}{k_M} \quad (3.18)$$

$$\delta_A = \max\left(\frac{k_p}{k_M}, \frac{k_M}{k_p}\right) \quad (3.19)$$

Equation 3.18 gives the factor  $\delta$  indicating whether the predicted permeability ( $k_p$ ) is greater or less than it was measured permeability ( $k_m$ ), so an average value of one indicates accuracy. Equation 3.19 indicates the absolute factor  $\delta_A$  equal to one or greater for predictions greater or less than  $k_m$ , so an average value of one indicates both accuracy and prediction. The tests were all performed in water at 20°C which is considered in the model of Judge et al. (*in press*). The corresponding hydraulic conductivity is easily computed as usual by taking into account the gravity  $g$  and kinematic viscosity  $\nu$  at a specified temperature for all permeability calculations.

$$K = \frac{kg}{\nu} \quad (3.20)$$

The uniform specimens have higher  $k$ , as expected due to their higher porosity. Higher grain sizes result in higher  $k$  values as expected because the surface area ratio is lower, the pore spaces are higher, and the tortuosity is usually slightly lower. The uniform specimens have a porosity about 2 percentage points higher than the well graded specimens, which are about 1.5 percentage points higher than the skew graded specimens. The good precision seen here is needed because small variations in porosity result in variations in permeability larger than the other factors that vary from test to test as shown in Table 3.2. The angular soil has more surface area per volume is slightly, but is more permeable because its higher void ratio has a stronger effect on  $k$ . The porosity

of each of the Tap Rock specimens was larger than the Brown Stone specimens of the same grain size gradation by about 1.5 percentage points which is likely due to its high angularity.

Table 3.2: Comparison of the effects of parameters on the permeability

		BS $C_{SH} = 6.8$ $d_{eff} \sim 16$ mm	BS $C_{SH} = 6.8$ $d_{eff} \sim 23$ mm	TR $C_{SH} = 7.6$ $d_{eff} \sim 16$ mm	TR $C_{SH} = 7.6$ $d_{eff} \sim 23$ mm
Well graded	$k_m = (m^2)$	3.4E-08	7.6E-08	5.7E-08	9.4E-08
	$n =$	0.375	0.367	0.392	0.380
	$r =$	1.39	1.29	1.24	1.21
Skew graded	$k_m = (m^2)$	6.5E-08	1.5E-07	5.8E-08	1.6E-07
	$n =$	0.389	0.374	0.399	0.398
	$r =$	1.26	1.14	1.28	1.14
Uniform graded	$k_m = (m^2)$	7.5E-08	1.7E-07	1.2E-07	1.9E-07
	$n =$	0.405	0.416	0.416	0.420
	$r =$	1.28	1.27	1.13	1.20

### 3.4 Conclusions

In consideration of the various factors presented and discussed in the previous section, an updated method of using the Kozeny-Carman equation for gravels is proposed that offers a method of determining the surface area of a specimen and incorporates the measured tortuosity into an empirically determined equation for the packing factor which has been theoretically investigated without conclusive results. The method presented of determining the surface area of two gravels is shown to give results that are very consistent and shape factors from two of the four examples provided by Fair and Hatch (1933). This suggests that this method works and can be used for a better approximation of the surface area of any specimen that does not match one of the four examples presented by Fair and Hatch (1933). The procedures presented can be used for coarse sands as well, but it is more difficult to determine the surface area and tortuosity of them.

The predicted permeability of the marbles reported by Judge et al. (*in press*) using the suggested packing factor of 5 without considering the tortuosity is still very close to the measured value using this new equation because the marbles have a low tortuosity. The predicted permeability of the stones tested in two orientations would be the same using this equation, but the measured  $k$  is not the same because  $\tau$  is much larger for these specimens with all other parameters equal. The effects of the grain size distribution, particle size, and porosity of two different soils tested in this study are shown with fine resolution in Table 3.2. Figure 3.6 shows the predicted versus measured  $k$  for the specimens (with an average of 1.2) which is considerably more precise than a factor of three which is considered to be a good correlation (Chapuis and Aubertin 2003) because of the high accuracy of the soil parameters and the permeability values measured using the model of Judge et al. (*in press*).

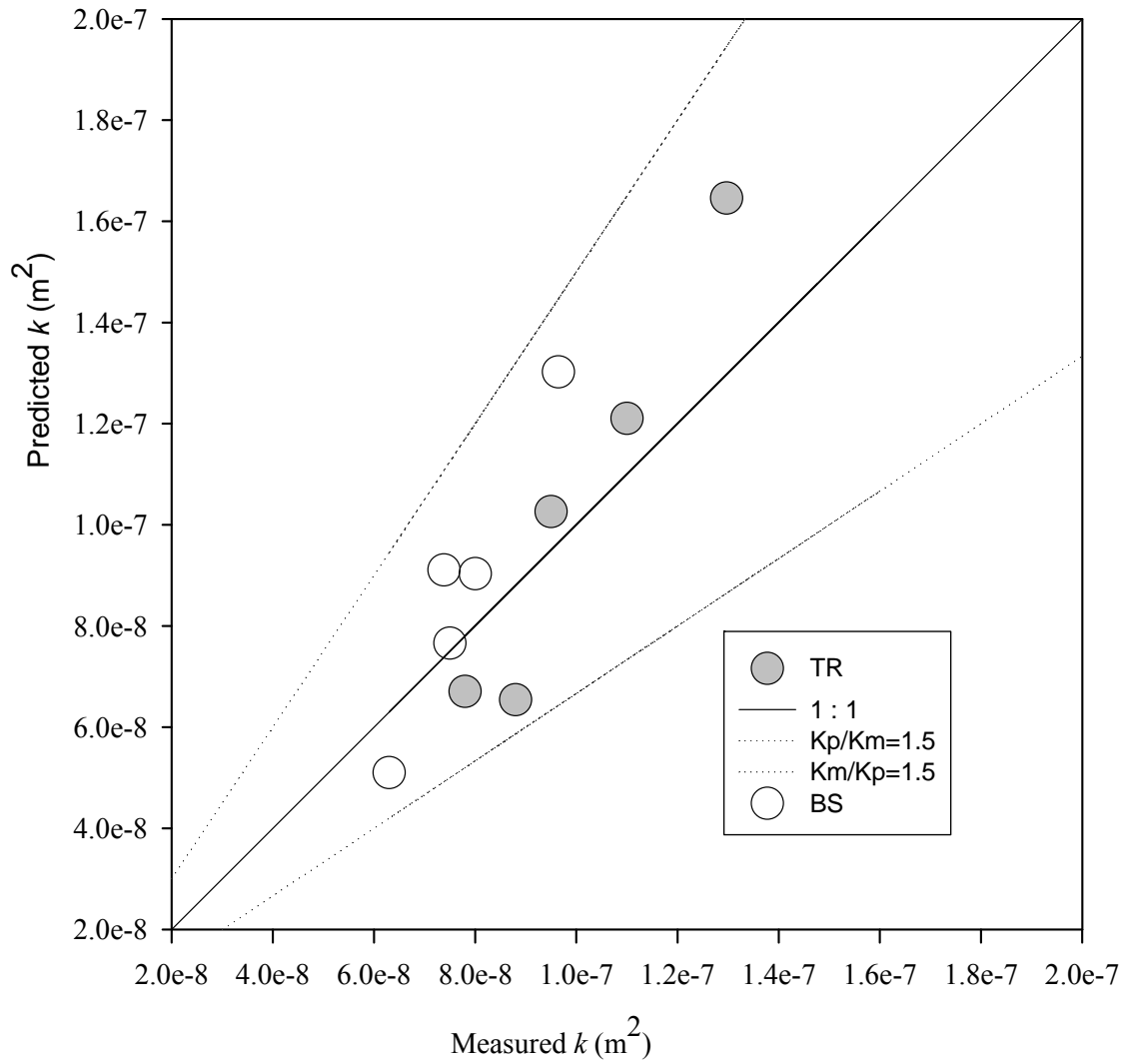


Figure 3.6: Predicted vs. measured permeability using Equation 3.1 and 3.17

## CHAPTER 4

### SLUG INTERFERENCE TESTS CONSIDERING THE EFFECTS OF WELLBORE STORAGE IN THE TESTED AND OBSERVATION WELLS

Slug interference tests were performed in pairs of wells installed with filter packs in a floodplain deposit of silty sand in Dedham MA by slug testing one well and measuring the response in both wells. These tests were run to determine the hydraulic conductivity and specific storage of the tested deposit. The hydraulic conductivity ranged from  $4 \times 10^{-6}$  to  $1.5 \times 10^{-5}$  m/s and the specific storage ranged from  $2 \times 10^{-5}$  to  $7 \times 10^{-4}$   $m^{-1}$ . The wellbore storage and filter pack effects on the measured pressure of both wells are modeled. The calibrated hydraulic parameters of the slugged and observation well matched well using the KGS Model by Hyder et al. (1994) only when modified to consider the filter pack and the wellbore storage in the observation well.

#### 4.1 Introduction and background

Slug testing is the most common method used to determine a quick estimate of the hydraulic conductivity of a natural formation. The results often do not match the results of pump tests or other available results so they are often considered a preliminary test. Pump test results represent a larger and more native volume of soil than slug test results and are more affected by infrequent conduits of high permeability, so higher values are usually obtained (Butler and Healey 1998). Incomplete well development and dynamic skins also have an effect on the results of slug tests which change over time if wells are tested again after the first time (Butler 1997). Leaking boreholes and improperly installed wells cause results to differ (Black 2010).



Butler (1997) summarized the methods of analysis of slug tests that affect the hydraulic conductivity results. Uncertainties of soil and formation properties in addition to well properties provide different soil properties for any analysis. Results are sometimes fit to type curves that are a function of hydraulic conductivity and specific storage and often times the data are forced to fit a curve that does not represent the soil properties so these two parameters are both compromised. Misinterpretation of the initial displacement of water is another reason that results may differ. The wellbore storage (water in the open well) and the wellskin (water in the highly permeable screen) illustrated in Figure 4.1 are not always considered in slug tests. Different methods of analysis provide results within about a half an order of magnitude of error, showing that either not everything is being considered in all solutions, or that some assumptions are wrong. Performing slug interference tests using the proper model and evaluating the data from one test utilizing two wells eliminates most of the problems listed.

Slug interference tests are performed by measuring and recording the water level in an observation well at a detectable distance (within about 10 meters), in addition to the well that was perturbed with a slug (slugged well) to determine the properties of the soil between the wells. The slug interference tests performed in this analysis consider wellbore storage (water in the open well) and wellskin (well filter pack) properties in both wells because they were both found to have a strong influence on the results. Prats and Scott (1975) showed that the effects of wellbore storage in the observation well manifest as a delay in time and diminishment of the peak of the head amplitude which results in underestimates of hydraulic conductivity and overestimates of specific storage. The effects of wellbore storage in the observation well on slug interference tests were

evaluated by Novakowski et al. (1989a) by considering the analysis of hypothetical tests performed with and without a packer to prevent flow in the observation well.

Slug interference tests were also evaluated analytically by Hyder et al. (1994) of the Kansas Geological Survey (KGS) with considerably more detail than other models. They considered partial penetration, the wellbore storage, anisotropy (when appropriate) and wellskin from the filter pack in the slugged well. They did not consider wellbore storage and wellskin were in the observation well because the model assumes that it is negligible or that the observation well was packed off to prevent flow. Presenting a model that evaluates the responses in the slugged and the observation well is a good way to confirm that the properties calculated are reliable because they both test a similar volume of soil at the same time. The hydraulic conductivity and specific storage are underestimated for the slug tests if the wellbore storage is not considered in the observation wells when significant (Novakowski 1989). The filter pack hydraulic conductivity is so high that the wellskin space behaves as if it is open. The change in head in the observation wells was found to be greater than the head outside the wellskin. This is because the surface area of the filter pack in contact with the formation is double that of the riser that was originally considered, so that is considered in the model presented in this paper.

Others have also evaluated slug interference tests in a semi-analytical way. Peres et al. (1989) developed a model for slug interference tests by transforming the data to equivalent pump test data. Spane (1996) used this model to show the effects of the aquifer thickness, hydraulic conductivity, anisotropy, storage, yield, and radial distance on the response of the water level. The Kansas Geological Survey (KGS Model) is a

semi-analytical model developed by Hyder et al (1994) to evaluate these tests because they are very sensitive to partial penetration and the wellskin of the slugged well. The KGS Model is used in this paper because it is simpler to use and it considers more soil and formation properties than the other methods, but it is modified to consider wellbore storage in the observation well using the equations developed by Novakowski (1989a) who considered the wellbore storage in the observation well using a semi-analytical model similar to that of Hyder et al. (1994).

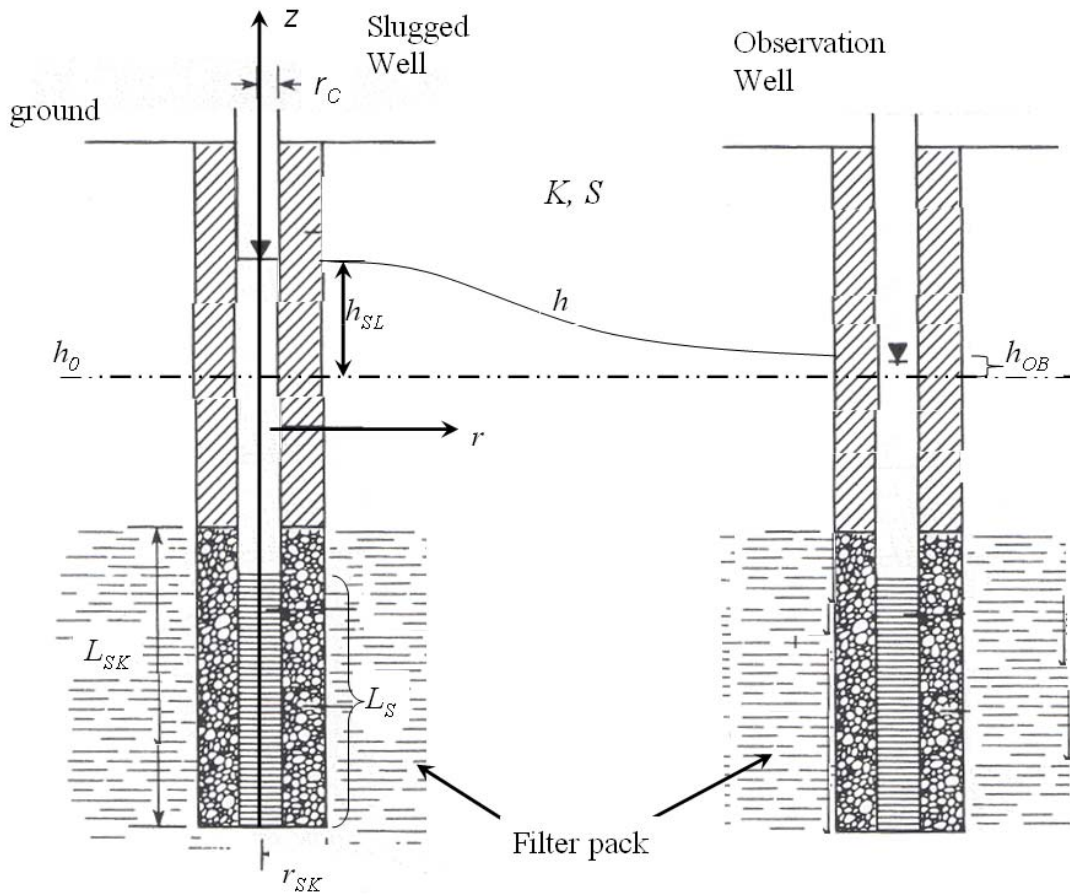


Figure 4.1: Definition Sketch

## 4.2 Model and boundary value problem

The problem of interest for slug interference tests is flow to or from the slugged well due to the recovery of a relatively instantaneous displacement of water, and the water pressure at a radial distance during a slug test. The boundary conditions were outlined by Hyder et al. (1994) who considered vertical flow and partial penetration for slug testing. The governing equation for radial flow into a well due to an instantaneous change of water level in a slightly compressible, unconfined aquifer neglecting vertical flow is given by Equation 4.1 where the hydraulic head in the aquifer ( $h$ ) is assumed to not change with the elevation above the impermeable bottom of the deposit ( $z$ ).

$$\frac{\partial^2 h}{\partial r^2} + \frac{1}{r} \frac{\partial h}{\partial r} = \frac{S}{K} \frac{\partial h}{\partial t} \quad (4.1)$$

The hydraulic conductivity of the formation is shown as  $K$ ,  $r$  is the radial distance from the centerline of the well,  $S$  is the specific storage of the soil, and  $t$  is time.

The initial and boundary conditions of Equation 4.1 are illustrated in Figure 4.1 which shows that there is no change in head before the start of the slug test and at a radial distance where  $h$  is equal to the initial head in the aquifer  $h_i$  and  $H_0$  is the applied slug.

$$h_i - h(r, z, 0) = 0 \quad (4.2)$$

$$h_i - h(\infty, z, t) = 0 \quad (4.3)$$

$$h_{SL}(0) = h_i + H_0 \quad (4.4)$$

The wellbore balance at the wellskin at the radius of the skin ( $r_{sk}$ ) for Equation 4.2 is given by Equation 4.5 where  $Q$  is the flow into the well,  $h_{SL}$  is the head in the slugged well, and  $r_{SK}$  is the radius of the skin.

$$2\pi r_{SK} L_{SK} \frac{\partial h}{\partial r} = Q + \pi r_C^2 \frac{dh_{SL}(t)}{dt} \quad (r=r_{SK}) \quad (4.5)$$

The length of the skin ( $L_{SK}$ ) is used in all analyses as opposed to the actual screen length because the skin is orders of magnitude higher in hydraulic conductivity. The continuity between the skin and the formation where auxiliary conditions differ by the effects of partial penetration are given for the slugged well during a slug test.

$$h_{SL}(z,t) = h(z,t) \quad r = r_{SK}, 0 \leq z \leq b, t > 0 \quad (4.6)$$

The head loss across the skin is negligible because the hydraulic conductivity of the skin is orders of magnitude greater than the deposit.

#### 4.2.1 Analytical model of slug interference tests

The model of Hyder et al. (1994) was used to evaluate the slug tests, but it was modified to consider the wellbore storage in the observation well considering the equations provided by Novakowski (1989) who did consider the wellbore storage in the observation well using a semi-analytical model. Also, the filter pack is considered to allow more water to enter the well by considering a mass balance of water entering the observation well. Hyder et al. (1994) neglected wellbore storage to calculate the head inside an observation well expressed in Laplace space. Doing so is equivalent to evaluating the head in the observation well as piezometric head shown here in Equation 4.7a which comes from Hyder et al. (1994) where  $C_{DS}$  is the wellbore storage factor,  $h_{SL}^*$  is the Laplace transform of the head in the slugged well ( $h_{SL}$ ),  $h^*$  is the Laplace transform of  $h$  in the aquifer,  $K_0(x)$  is a Modified Bessel function of the zero order,  $K_1(x)$  is a Modified Bessel function of the first order,  $p$  is the Laplace transform coefficient, and  $r_D$  is the dimensionless radial distance  $r/r_{SK}$ . Equation 4.7a can be used for the slugged well by setting  $r_D=1$  or to evaluate  $h$  in the aquifer at  $r_D>1$ .

$$h_{SL}^*, h_A^* = \frac{\Omega_2}{[1 + p\Omega_1]} \quad (4.7a)$$

$$\Omega_1 = p^{-1/2} C_{DS} \frac{K_0(p^{1/2})}{K_1(p^{1/2})} \quad (4.7b)$$

$$\Omega_2 = C_{DS} \frac{K_0(r_D p^{1/2})}{K_1(p^{1/2})} \quad (4.7c)$$

$$C_{DS} = \frac{\pi c^2}{2\pi s_{SK}^2 SL_{SK}} \quad (4.7d)$$

Equation 4.7a is easily evaluated using the Stepest algorithm in a visual basic code through Microsoft Excel provided by Esling and Keller (2009). Equation 4.7a is edited in this paper to reflect the wellbore storage by exploring the LaPlace equations used by Novakowski (1989b). This provides the head in the well, which differs from the water pressure in the soil at that radial distance from the slugged well.

Novakowski (1989b) considered the same problem that Hyder et al. (1994) considered, giving the equations for hydraulic head in the slugged well, the aquifer, and the observation well. He presented type curves based on theoretical results evaluated using an analytical model that is used to calculate the specific storage and hydraulic conductivity. His solution considers the hydraulic head in an observation well with and without wellbore storage. The solution without wellbore storage gives the head in the aquifer (piezometer head) given by Equation 4.7a. His solution for the head in the observation well considering wellbore storage is given by Equation 4.8a where  $C_{DO}$  is the wellbore storage factor in the observation well (Equation 4.8d), which is the same as  $C_{DS}$  in this study because the radii of the slugged and observation wells are the same.

$$h_A^*, h_{OB}^* = \frac{K_0(r_D p^{1/2})K_1(p^{1/2})}{-p^{3/2}C_{DO}[K_0(r_D p^{1/2})]^2 + \xi_1\xi_2} \quad (4.8a)$$

$$\xi_1 = [C_{DO} p^{1/2} K_0(p^{1/2}) + K_1(p^{1/2})] p^{1/2} \quad (4.8b)$$

$$\xi_2 = \frac{C_{DS} p^{1/2} K_0(p^{1/2}) + K_1(p^{1/2})}{C_{DO}} \quad (4.8c)$$

$$C_{DO} = C_{DS} \quad (4.8d)$$

Equation 4.8a is used with Equations 4.8b and 4.8c and rewritten with  $C_{DS}, p^{1/2}$ , and  $K_I(x)$  to show all terms.

$$h_{OB}^* = \frac{\frac{C_{DS} K_0(r_D p^{1/2})}{p^{1/2} K_1(p^{1/2})}}{\frac{-p C_{DS} C_{DO} K_0(r_D p^{1/2})^2}{K_1(p^{1/2})} + \frac{p^{1/2} C_{DO} K_0(p^{1/2})}{K_1(p^{1/2})^2} [p^{1/2} C_{DS} K_0(p^{1/2}) + K_1(p^{1/2})]} \quad (4.9)$$

Equation 4.9 is then rewritten using Equations 4.7b, 4.7c, 4.7d, and 4.8d.

$$h_{OB}^* = \frac{\Omega_2}{-\Omega_2^2 p^2 + \Omega_1^2 p^2 + 2\Omega_2 p + 1} \quad (4.10)$$

Equation 4.11 evaluates a case of Equation 9 as head in a piezometer ignoring wellbore storage to ensure that it matches the solution of Hyder et al. (1994) by setting  $C_{DO}$  to zero.

$$h_{OB}^* = \frac{\frac{C_{DS} K_0(r_D p^{1/2})}{p^{1/2} K_1(p^{1/2})}}{p \frac{p^{1/2} C_{DS} K_0(p^{1/2})}{K_1(p^{1/2})} + 1} \quad (4.11)$$

Equation 4.11 can be rewritten using simplified terms and is in fact equal to Equation 4.7a, which justifies using Equation 4.10 to solve for the head in the observation well considering the wellbore storage in the observation well.

Equation 4.10 gives the head in an observation well considering that the screen and casing of the observation well have the same radius. The hydraulic conductivity of the filter pack is several orders of magnitude larger than the formation which results in an

equivalent radius that is double the radius of the well size. This causes twice as much water to enter the observation well for sudden pressure changes due to a slug test, which means that the head in the well is double that given by Equation 4.10 which is rewritten to reflect this by considering this factor of two in Equation 4.12.

$$h_{OB}^* = \frac{2\Omega_2}{-\Omega_2^2 p^2 + \Omega_1^2 p^2 + 2\Omega_2 p + 1} \quad (\text{considering the skin}) \quad (4.12)$$

The effects of Equation 4.12 on the results on the hydraulic conductivity and specific storage values calculated from the data in the observation wells are shown in the results section. Equation 4.12 is used for the results, but Equations 4.7a and 4.10 are presented in the discussion to show that they yield results from the two wells that are not consistent.

### **4.3 Site description and well arrangement**

The observation wells are made of 5-cm diameter PVC construction with 10-cm diameter sand packs outside the 1.5 meter long well screens. Above the sand packs are bentonite seals up to the ground surface where the wells are finished with locked steel casings and concrete pads. Most wells were installed in clusters spaced about a meter apart with 1.5 meter screens at different vertical depths, to assess the hydraulic head and difference in the water quality in the different soil layers. Pairs of wells were installed about a meter apart in each cluster in the floodplain deposit to allow for uninterrupted monitoring of the well while the wells were pumped monthly.

Bedrock at the Dedham site is overlain by basal till turning to sand, which forms the confined sandy aquifer used to supply water to the towns of Dedham and Westwood. The lake bed sediments above this are mostly formed of silt with varying amounts of fine sand and clay. Covering all of the other underlying strata is a deltaic floodplain deposit



consisting of silty sand (LaMesa 2008). Figure 4.2 shows the location of the site from LaMesa (2008). The details on the hydraulic properties and dimensions of the wells based on previous slug tests evaluated using Bouwer and Rice (1976) are provided in Table 1 where  $L_S$  is the length of the screen and  $k$  is the permeability.

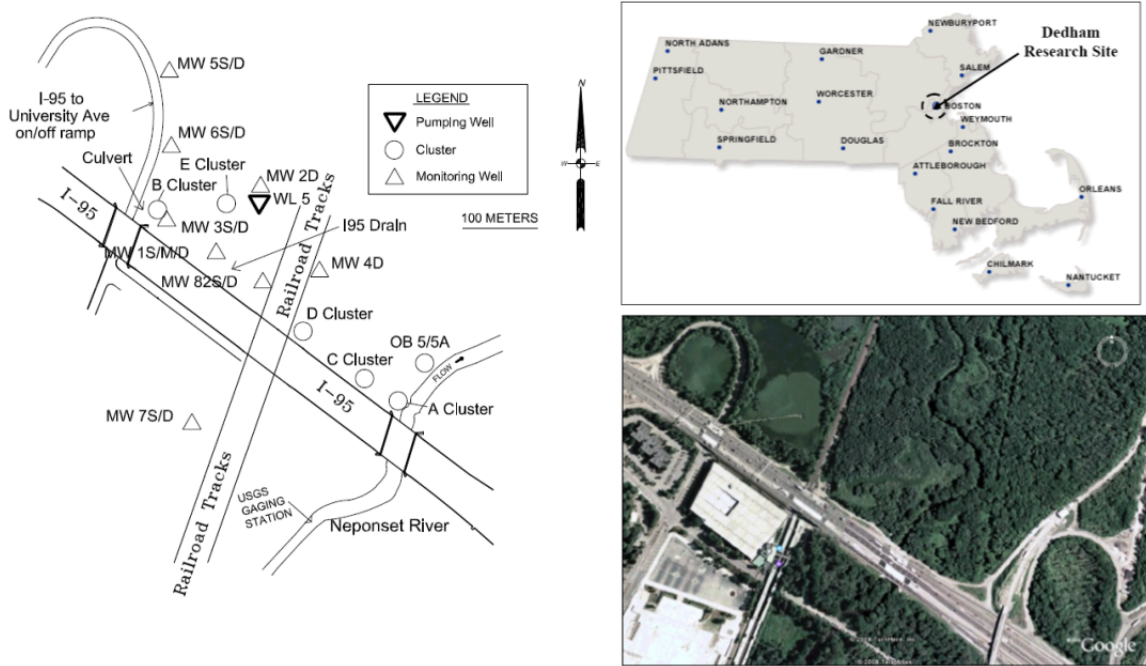


Figure 4.2: Dedham site location from LaMesa (2008)

Table 4.1: Dimensions of the wells and hydraulic conductivity based on previous slug tests by LaMesa (2008).

	$r$ (m)	$b$ (m)	$L_{sk}$ (m) =
Cluster A	1.3	20.4	2.6
Cluster C	0.55	24.1	2.3
Cluster D	0.82	23.5	2.6
For all wells:			
$r_C$ (m) =	0.008		
$r_{SK}$ (m) =	0.016		
$L_S$ (m) =	1.52		

### 4.3.1 Methods of performing tests

Water levels were measured before and after the slug tests to establish the static head. Traditional slug tests were run by either inserting (slug-in test) or extracting (slug-out test) a solid aluminum rod to force a displacement in the equilibrium water level in the well. Small or large slugs which displace 0.3 m or 1 m were used for the tests. The results of all tests yielded identical hydraulic parameters regardless of these considerations so they were all normalized and reported as positive head as shown in Figure 4.1.

The slugged and observation wells were instrumented with Level Troll 500 Pressure Transducers (In Situ Inc., Fort Collins, Colorado) to record temperature and pressure readings at a rate of 0.5 to 1 Hz with a reported accuracy of 0.07 kPa. The well was allowed to come to static equilibrium with the transducer in it and then the aluminum rod was inserted to initiate the slug-in test. After the well was at least 90% recovered back to its static water level; the test was stopped and the slug was removed to initiate the slug-out test. The data were then uploaded to a laptop.

### 4.3.2 Results

The wellbore storage and wellskin both have an effect on the head in slugged and observation wells during a slug test. The results vary enough to yield values of specific storage and hydraulic conductivity that can differ by a factor of at least two if these effects are not considered. The slug test results are listed in Table 4.2 and the calibrations of the slugged well and the observation well using Equation 4.12 are shown in Figure 4.3. The results from LaMesa (2008) are shown in Table 4.3. The data from each well were each calibrated to the model with the same values for  $K$  and  $S$ . The compressibility ( $\alpha$ )

of the silty sand is within the range of sand of  $10^{-9}$  to  $10^{-7}$  Pa<sup>-1</sup> (Freeze and Cherry 1979) using Equation 4.13 assuming porosity ( $n$ ) of 0.4 where  $g$  is gravity,  $\beta$  is the compressibility of water equal to  $4.4 \times 10^{-10}$  Pa<sup>-1</sup>, and  $\rho_w$  is the density of water.

$$\alpha = \frac{S}{g\rho_w} - n\beta \quad (4.13)$$

The hydraulic conductivity is lower by a factor of about 1.5 compared to the results of LaMesa (2008) who considered the Bouwer and Rice (1976) method except for the A cluster. The specific storage is lower for the less permeable Cluster D as expected because the compressibility is typically lower for less permeable soil. Cluster A is an exception here as well, suggesting that the results may subject to error. The observation well is much more sensitive to the calibrations than the slugged well, which makes this such a good test to evaluate. Lower  $S$  values drive the peak  $h$  value of the observation well up and towards the start of the test a bit while higher  $K$  values drive the peak  $h$  value to the left.

Table 4.2: Slug test calibrations determined considering the presented model using Equation 4.12 for both wells and the other equations for the observation well.

	Eq. 4.12	Eq. 4.10 (no skin)	Eq. 4.7a (no skin or wellbore storage)	Eq. 4.12	Eq. 4.10 (no skin)	Eq. 4.7a (no skin or wellbore storage)	Eq. 4.12
Well Cluster:	C	C	C	D	D	D	A
K (m/s)	9.1E-06	9.1E-06	6.1E-06	3.7E-06	1.8E-06	1.1E-06	1.5E-05
S (m <sup>-1</sup> )	6.6E-04	1.6E-04	3.3E-04	1.2E-04	9.8E-06	4.9E-05	2.3E-05
Compressibility (Pa <sup>-1</sup> )	6.7E-08	1.7E-08	3.3E-08	1.3E-08	8.3E-10	4.8E-09	2.2E-09

Table 4.3: Slug test results from LaMesa (2008) using the Bouwer and Rice method

	$K$ (m/s)
Cluster A	1.5E-05
Cluster C	1.2E-05
Cluster D	6.1E-06

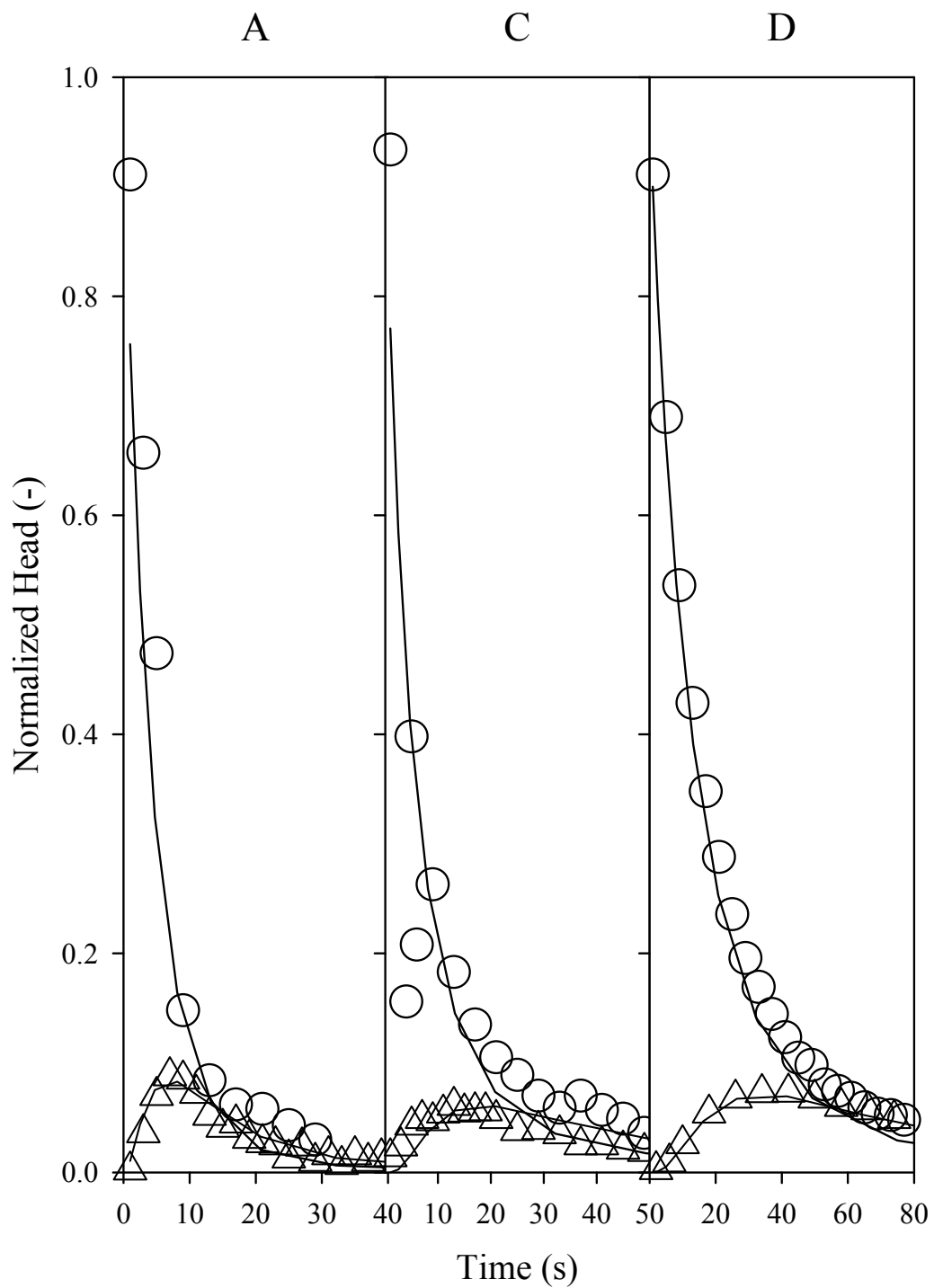


Figure 4.3: Slug test results in the slugged and observation wells using the model presented in Equation 4.12 for the observation wells

#### 4.4 Discussion

The KGS Model by Hyder et al. (1994) does not consider wellbore storage or the wellskin in the observation well like it does in the slugged well. This original KGS model is considered here in order to show that this needs to be considered in both wells. Dedham Clusters C and D are evaluated using three models here to demonstrate this. Cluster A is omitted because the results are less sensitive:

1. The KGS model given by Equation 4.7a which does not consider the wellskin or wellbore storage in the observation well.
2. The inclusion of the wellbore storage in the observation well to the KGS Model (but not the wellskin) as described in Equation 4.10.
3. The current model considering wellbore storage and the wellskin using Equation 4.12, which is used to present the results.

Figure 4.4 shows all three observation well equations presented in Table 4.2 to model the head in the observation well using the  $K$  and  $S$  values calibrated from the tests shown in Figure 4.3. This demonstrates that the current model is needed for a good fit of the data because the other models do not fit the measured data using the calibrated  $K$  and  $S$  values. The alternative considerations do not fit the measured data as seen in Figure 5. The  $K$  and  $S$  values calibrated using Equation 4.7a and 4.10 in Table 2 had a good fit, but do not match the slugged well data, much like is seen in Figure 4.4. The specific storage values used to fit are lower by a factor of up to fifty. It is clear again that the current model gives a better fit to the measured data than the other models.

The radial distance was considered with half and double the measured distance to determine the sensitivity of the results on the horizontal distance between well screens.

The radial distance was determined by measuring the distance from one well to another, assuming that each well was installed without any inclination. An inclination of one degree results in the screen of a well being located 1.7% of its depth in the opposite direction of inclination. A well that is screened at 50 feet will have a screen that is 0.87 feet in the direction of inclination, which is about 20-30% of the measured horizontal distance between the tops of risers in this study. A value of half the radial distance would underestimate  $S$  by about an order of magnitude and slightly overestimate  $K$ . Double the value of the radial distance would have the opposite effect on  $S$  and  $K$ . This may be a cause of error in the A cluster where the fit presented in Figure 4.4 is compromised a bit.

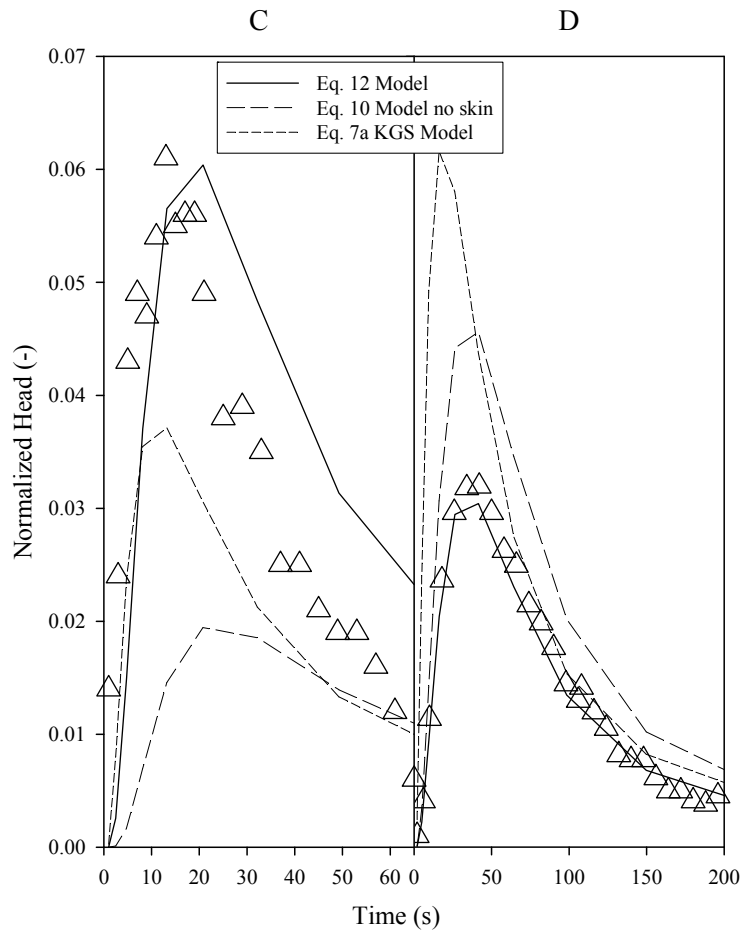


Figure 4.4: The three observation well models considered in Table 4.2 using the hydraulic conductivity and specific storage values calibrated using Equation 4.12

#### **4.5 Summary and Conclusions**

The slug test results from the slugged and observation wells using the presented model yielded similar and plausible values for hydraulic conductivity and specific storage considering the wellbore storage and the filter pack. The results of the two wells considered would be inconsistent if the wellbore storage and the filter pack were not considered in the model as shown in Table 4.2 and illustrated in Figure 4.4. Erroneously low values of specific storage would not even fit the curve if the filter pack radius and wellbore storage were not considered in some cases. The water level responses of both wells are affected by the same volume of soil, about 1 meter around the slugged well so they should yield similar results. The slug tests give consistent results of the specific storage and hydraulic conductivity surrounding the well within the effective radius of the slug tests, which is about one meter.

## CHAPTER 5

### SUMMARY AND CONCLUSIONS

The primary objectives of this dissertation were to find better ways to perform hydraulic conductivity tests on highly permeable coarse grained soils using a new laboratory device, to use the results to improve a current grain size to hydraulic conductivity correlation, and present an improved method of analyzing slug interference tests. These objectives were met through three chapters that present new methods of performing hydraulic conductivity tests and evaluating the results. A brief overview of the most important results of these chapters is presented below as an overview of the results presented in this dissertation.

Chapter 2 presented a permeameter designed to determine the hydraulic conductivity of gravels ranging from 0.1 to 2 m/s. A model was developed that calibrates the hydraulic conductivity and also provides the tortuosity. The hydraulic conductivity of the marbles calculated using the Kozeny-Carman equation was within 5% of the calibrated value and the repeatable results followed Darcy's law.

Chapter 3 presented an updated method of using the Kozeny-Carman equation for gravels is proposed that offers a method of determining the surface area of a specimen and incorporates the measured tortuosity and measured hydraulic conductivity into an empirically determined equation for the packing factor. This has been theoretically investigated by others without conclusive results so the model was improved by considering the tortuosity. The predicted versus measured hydraulic conductivity for the specimens was within an average of 1.2 using this consideration, which is more precise than the factor of three which is considered to be a good correlation (Chapuis and Aubertin 2003).



Chapter 4 presented the slug test results from the slugged and observation wells using the presented model yielded similar and plausible values for hydraulic conductivity and specific storage considering the wellbore storage and the filter pack. The results of the two wells considered would be inconsistent if the wellbore storage and the filter pack were not considered. The water level responses of both wells are affected by the same volume of soil, about 1 meter around the slugged well so they should yield similar results. The slug tests give consistent results of the specific storage and hydraulic conductivity surrounding the well within the effective radius of the slug tests, which is about one meter.

## **APPENDIX: LIST OF PRESENTATIONS**

1. Judge, A. December (2011). Hydraulic Conductivity of Gravel Samples using a Modified Permeameter. Poster presentation at AGU - Annual Meeting, San Francisco CA, 5 December 2011.
2. Judge, A. December (2012). Hydraulic Conductivity of Gravel Samples using a Modified Permeameter. Oral presentation at UMass Amherst, Northeast Geotechnical Graduate Research Symposium, 26 October 2012.
3. Judge, A. (2013). Hydraulic Conductivity of Gravel Samples using a Modified Permeameter. Oral presentation at GSA Northeastern Section - 48th Annual Meeting 18 March 2013.

**Introduction**

- permeameter is designed to perform tests on very coarse gravel to determine its hydraulic conductivity with fine resolution.
- Optic framework gravel interbedded in channels and fluvial deposits is of interest, where field tests performed in wells screened in these formations may reflect hydraulic properties of a combination of other deposits of soil.
- Research on laboratory hydraulic conductivity testing of gravel more permeable than 10 cm/s is limited because the responses are difficult to measure and often have precision within only 20% among multiple tests.

**Procedures**

- Specimens of saturated gravel have 200 Pa pneumatic pressure applied to the free surface in a riser connected above it, depressing the water level 2 cm.
- The pressure is then released and the underdamped responses that are observed in the riser are similar to pneumatic slug tests performed in very permeable soils as noted by Van der Kamp (1976), Zienkiewicz and McGuire (1994) and Oosthoff et al. (2005), who evaluated the friction and inertia present in these tests.

**Theory**

- The results of the tests performed in this study are evaluated using underdamped slug testing theories with some modification.
- The period of the oscillations is governed by the inertia of the water column ( $L_r$ ), the length of riser and cylinder multiplied by the ratio of the velocity changes throughout the cylinder to follow Euler's momentum equation of motion in unsteady form.
- Unsteady head losses in the permeameter and frictional losses in the soil dampen the amplitude of the water column in the riser over time, expressed by the damping frequency ( $\alpha$ ).
- The sum of the minor losses at the contraction at the base of the cylinder and the interface of the riser and cylinder ( $F_{r,c}$ ) is calibrated to the results of tests performed without soil, and is considered with the total losses of tests with soil ( $F$ ) to calculate the hydraulic conductivity.
- The hydraulic conductivity equation is found by vertically integrating the pressure gradient to the transducer from both the free surface in the riser and the outside static water level, and equating the equations.

$$\frac{d^2\eta}{dt^2} + 2\alpha\frac{d\eta}{dt} + \omega^2\eta = 0 \quad (0 < t < L_r)$$

$$\eta = \frac{1}{\omega} \exp\left(-\frac{\alpha t}{2}\right) \left[ \frac{v_0}{\omega} \sin\left(\frac{\omega t}{2}\right) + \frac{v_0}{\omega} \cos\left(\frac{\omega t}{2}\right) \right]$$

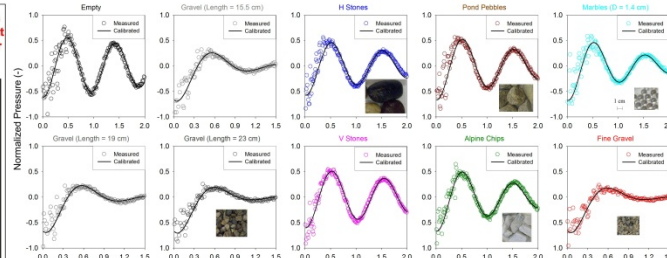
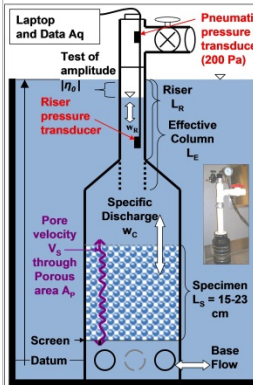
$$L_r = L_r + (L_r - L_r) \left( \frac{v_0}{v_0} \right) + \left( \frac{v_0}{v_0} \right) \left( \frac{v_0}{v_0} \right)$$

$$\alpha = \frac{2}{L_r} \left( \frac{F_{r,c}}{\rho g} + \frac{F}{\rho g} \right)$$

$$k = \frac{D_r}{D_r} \left( \frac{v_0}{v_0} \right) \left( \frac{v_0}{v_0} \right)$$

$$P = \rho g \eta + \rho g \frac{L_r - D_r}{L_r} \eta$$

$$L_r \rho \frac{d^2\eta}{dt^2} + 2 \rho g \frac{L_r - D_r}{L_r} \eta$$



**Results**

- Tests were conducted on several kinds of gravel which include perfectly spherical marbles (d = 1.4 cm) with a known specific surface and void ratio.
- Stones were tested with the long direction in the same direction as the vertical flow (V Stones), and also against it horizontally (H Stones).
- Although the volumetric void ratio and grain size distributions are the same for each, the tenacity of the flow of water is greater for the horizontally aligned specimens, resulting in a lower hydraulic conductivity.
- The average error in head values determined from the model throughout the tests is 1 mm from the measured values, or about 6% of the initial displacement of 2 cm.
- Tests performed on the three gravel specimens are within 5% of the average value.
- Tests performed on the marbles reveal higher values than grain size models.

	empty	V stones	H Stones	A. Chips	P. Pebbles	marbles	gravel	gravel	gravel	fine gravel
$L_r$ (m)	0.220	0.281	0.248	0.244	0.249	0.247	0.242	0.247	0.253	0.243
$\omega$ (s <sup>-1</sup> )	0.43	0.63	0.87	1.17	0.95	1.50	3.79	4.20	4.74	4.99
Porosity $n$ (-)	1.00	0.31	0.40	0.48	0.43	0.44	0.44	0.44	0.44	0.35
Initial Displacement $\eta_0$ (m)	0.017	0.050	0.051	0.054	0.051	0.052	0.054	0.054	0.057	0.055
Error $\delta$ (%)	1.8-03	1.8-03	2.8-03	1.8-03	2.8-03	1.8-03	1.8-03	1.8-03	1.8-03	2.8-03
Error $\delta$ (%)	8.1%	3.8%	7.1%	5.8%	7.1%	8.7%	8.9%	4.9%	4.9%	6.1%
Specimen Length $L_s$ (m)	0.105	0.165	0.200	0.200	0.190	0.190	0.190	0.190	0.230	0.155
Losses $F$ (-)	3.6	4.0	5.5	10	9.0	16	66	68	75	82
Soil Losses $F$ (-)	0.4	1.9	6.4	5.4	12	53	64	72	77	77
Permeability $k$ (m <sup>2</sup> )	1E-06	2.5E-07	1.2E-07	1.8E-07	7.5E-08	2.0E-08	2.2E-08	2.3E-08	1.5E-08	1.5E-08
Hydraulic Conductivity $K$ (m/s)	11	2.4	1.2	1.5	0.72	0.20	0.21	0.22	0.22	0.15
Hydraulic Conductivity $K_0$ (m/s)	8	1.9	0.92	1.2	0.56	0.15	0.16	0.17	0.17	0.11
Linearized Velocity $w_c$ (m/s)	0.052	0.083	0.079	0.057	0.052	0.047	0.032	0.031	0.032	0.030

**References**

Oosthoff, J.W., Oosthoff, D.J., Oosthoff, P.J., Marlowe, J., 2005. A Closed Form Slug Test Theory for High Permeability Aquifers. Groundwater 43(1): 1-10.

Van der Kamp, G., 1976. Determining Water Permeability by Means of Slug Test Theory. In: "Underground Geology".

Zienkiewicz, J.C., McGuire, R.V., 1994. Research on Laboratory Hydraulic Conductivity Testing of Gravel More Permeable than 10 cm/s. In: "Proceedings of the 1994 International Conference on Soil Mechanics and Foundation Engineering".

MassDOT Highway Division, 2008. Final Test Report: Under-Integrating Services Agreement 080805. The views, opinions, and findings contained in this document are the Author's and do not necessarily reflect the official view or policies of MassDOT.

**Hydraulic Conductivity of Gravel  
Samples using a Modified  
Permeameter**

Aaron Judge  
University of Massachusetts  
Amherst, MA

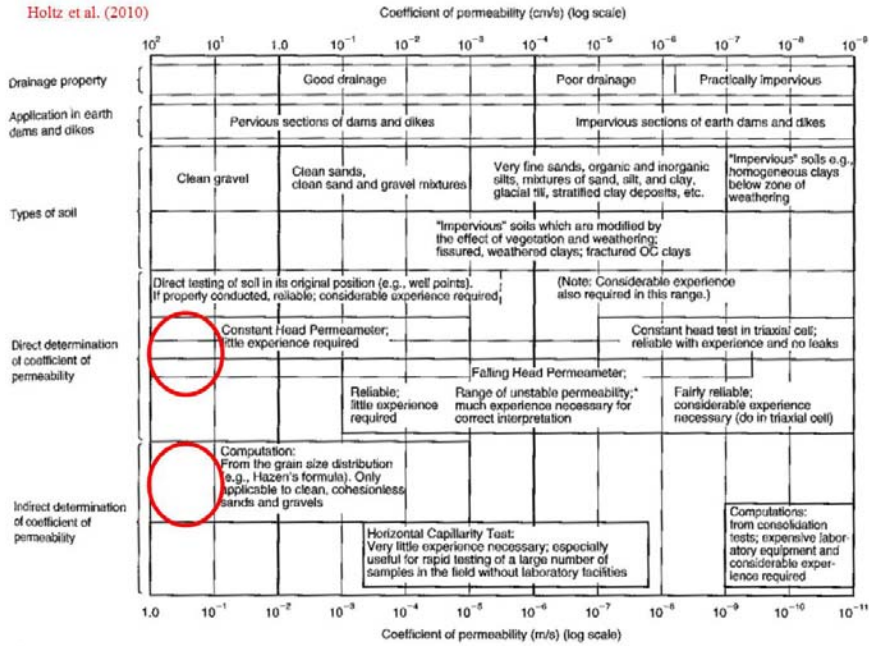
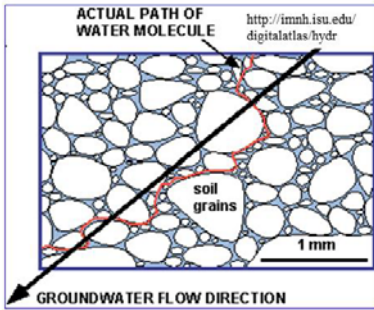
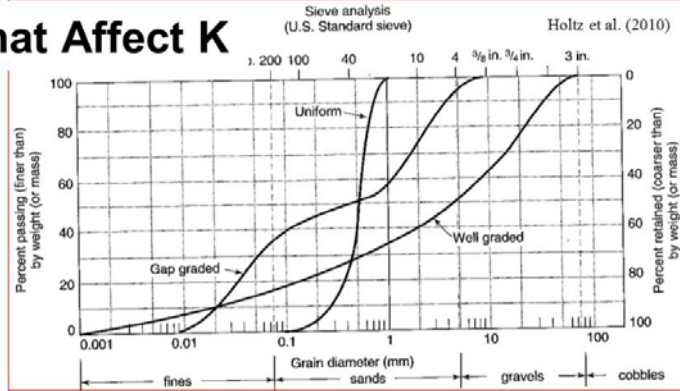


FIGURE 7.7 Permeability, drainage, soil type, and methods to determine the coefficient of permeability (after A. Casagrande, 1938, with minor additions).

# Properties that Affect K

- Specific Surface and Grain Size Distribution
- Porosity, Tortuosity
- Roundness and Sphericity
- Fluid viscosity



<http://www.agcsa.com.au/>

						<b>High Sphericity</b>	
							<b>Medium Sphericity</b>
							<b>Low Sphericity</b>
Very Angular	Angular	Sub-Angular	Sub-Rounded	Rounded	Well Rounded		

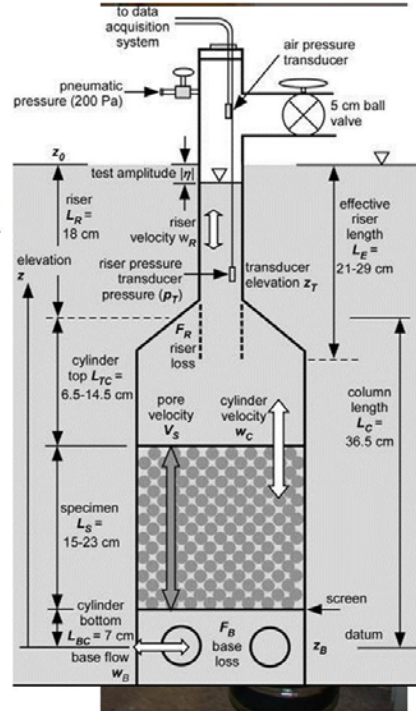
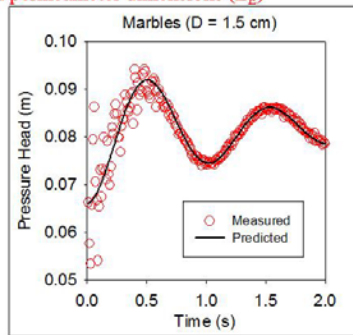
## Approach

- The water level in a riser above a specimen of saturated soil in a cylinder is oscillatory when pressure is released.

A Bessel function of the water level over time calibrates the head losses and  $K$  to measured pressure.

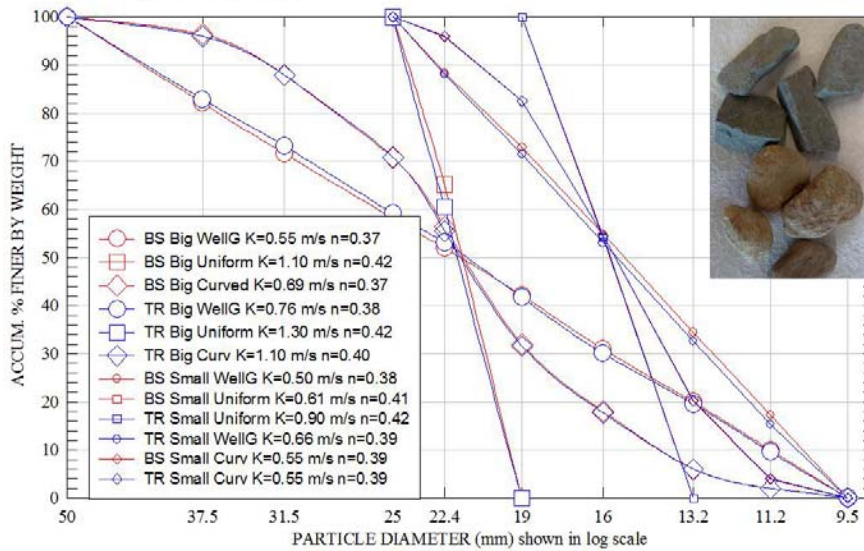
$$\eta = \eta_0 \exp\left(-\frac{\omega t}{2}\right) \left[ \cos\left(t \sqrt{\frac{g}{L_E} - \frac{\omega^2}{4}}\right) + \frac{\sin\left(t \sqrt{\frac{g}{L_E} - \frac{\omega^2}{4}}\right)}{\sqrt{\frac{4g}{\omega^2 L_E} - 1}} \right]$$

- The pressure is shown as a linearized function of acceleration, velocity, and position.
- Optimized head losses and hydraulic conductivity ( $\omega$ )
- Measured permeameter dimensions ( $L_E$ )



Higher K values found with:

1. Higher grain size
2. Uniform distribution (*in all but one shown*)
3. Higher void ratio



Preliminary Results of Brown Stones and Tap Rock normalized to 10°C. Tap Rock (TR, top of picture) and Brown Stone (BS, bottom of picture) shown are > 25 mm.



## Empirical Correlation

- Estimates within three times of  $K$  are accepted as a good grain-size analysis.

$$k = \left(\frac{d_m^2}{180}\right) \left(\frac{e^3}{1+e}\right) \text{ Kozeny-Carman Model}$$

← Shape, packing, and grain size distribution

- The effective grain size diameter  $d_m$  is ambiguous in the literature ( $d_{10}$ ,  $d_{50}$ ).

$$k_{GSM} = \left[ c_1 d_{10}^2 + c_2 d_{30}^2 + c_3 d_{70}^2 + c_4 d_{90}^2 \right] \frac{1}{\tau^2} \left(\frac{e^3}{1+e}\right)$$

$$\delta = \sum |k_{Measured} - k_{Pred}|$$

- The K-C Model gave the same  $K$  as my tests for the marbles.

For soil = 1 To 20

$$k_{pred}(\text{soil}) = \sum D_{10-90} [c_1 D_{10}(\text{soil})^2 + \dots + c_4 D_{90}(\text{soil})^2] (\text{void ratio exp}) / \tau^2$$

$$\text{delta}(\text{soil}) = \text{Abs}(k_{meas}(\text{soil}) - k_{pred}(\text{soil}))$$

Next soil

- The  $c$  coefficients are calibrated to the results of all tests by minimizing the error.

	$n_{min}$	$n$	$n_{max}$	$D_{10}$ (mm)	$D_{30}$ (mm)	$D_{70}$ (mm)	$D_{90}$ (mm)	$k$ meas (m2)	$k$ pred (m2)	error	abs error
D MultMin				1.4E-03	5.0E-05	1.8E-04	4.1E-05				
D MultMax				4.1E-03	1.5E-04	5.3E-04	1.2E-04				
D Multiplier				2.1E-03	7.5E-05	2.7E-04	6.1E-05				
diff				25%	25%	25%	25%				
BS BigLog	0.35	0.37	0.44	11.2	16.0	30.0	42.0	7.4E-08	7.7E-08	-4%	4%
BS BigCurv	0.35	0.37	0.44	14.2	18.9	24.8	32.0	9.3E-08	8.9E-08	4%	4%
BS BigU	0.35	0.42	0.44	19.5	20.6	22.9	24.0	1.5E-07	2.1E-07	-41%	41%
BS SmallLog	0.36	0.38	0.42	10.2	12.9	18.6	22.5	6.7E-08	4.7E-08	30%	30%
BS SmallCurv	0.36	0.39	0.42	11.8	13.9	17.0	20.3	7.4E-08	6.3E-08	14%	14%
BS SmallU	0.36	0.40	0.42	13.8	14.6	16.7	18.4	8.2E-08	9.4E-08	-15%	15%
									sum:	10%	19%

# Questions?

Thanks to

- Dr. DeGroot and  
Dr. Ostendorf
- Fellow Grad  
Students
- Friends and  
Family
- Mass Highway

# Hydraulic Conductivity of Gravel Samples using a Modified Permeameter

Judge, A., DeGroot, D.J., and Ostendorf, D.W.  
Department of Civil and Environmental Engineering,  
University of Massachusetts, Amherst, MA 01003



Northeastern Section - 48th Annual Meeting  
Geological Society of America

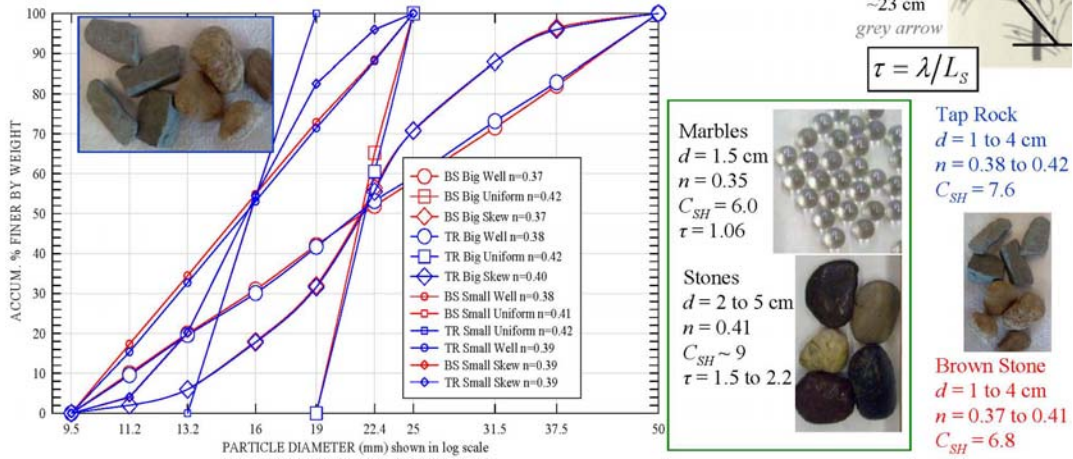
[T34. Engineering Geology in the 21st Century](#)

Paper No. 21-2 Presentation Time: 1:55 PM

[judge@ecs.umass.edu](mailto:judge@ecs.umass.edu)

## Gravels tested and their properties

- Gravels are used in roadway construction, drainage curtains, and railroad ballast. Often a minimum and maximum rate of drainage are required for a designed material or use of a natural formation.
- Hydraulic Conductivity ( $K$ ) is affected by surface area ( $SA$ ), porosity ( $n$ ), and tortuosity ( $\tau$ ) which were measured and determined from theory presented by Judge et al. (2013) for gravels.
- Spherical marbles and anisotropic stones were tested by Judge et al. (2013) in developing high- $K$  testing where  $K = 0.2$  to  $2$  m/s.
- Two sets of coarse gravels (**Tap Rock** and **Brown Stone**) with different shape factors ( $C_{SH}$ ) were arranged to 12 specimens to evaluate the Kozeny-Carman equation and empirically determine the packing factor as a function of  $\tau$  using the measured  $K$ .



Judge, A., Ostendorf, D.W., DeGroot, D.J. and Zlotnik, V.A. (2013). "A Pneumatic Permeameter for Transient Laboratory Tests." *Journal of Hydrologic Engineering*. In Press.

- Specimens of saturated gravel have 2 cm of pneumatic pressure applied depressing the free surface in the riser.
- The pressure was then released causing underdamped responses similar to pneumatic slug tests performed in very permeable soils by Zlotnik and McGuire (1994) and Ostendorf et al. (2005).

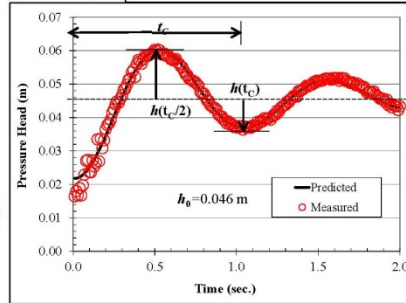
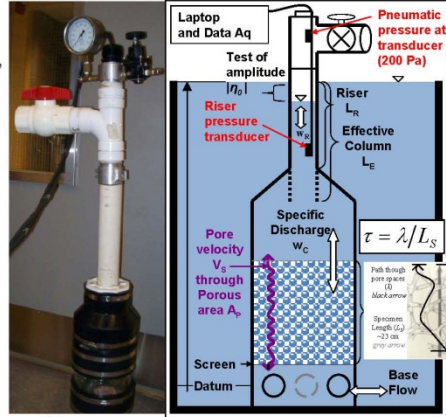
•The measured water pressure was calibrated to the model of Judge et al. (2013) giving  $K$  and  $\tau$  through the soil by integrating the pressure changes considering acceleration, velocity, and position.

• $K$  dampens the oscillations following Darcy's law with laminar flow.

• $\tau$  increases  $L_E$  which affects  $t_C$  which is needed for a good calibration.

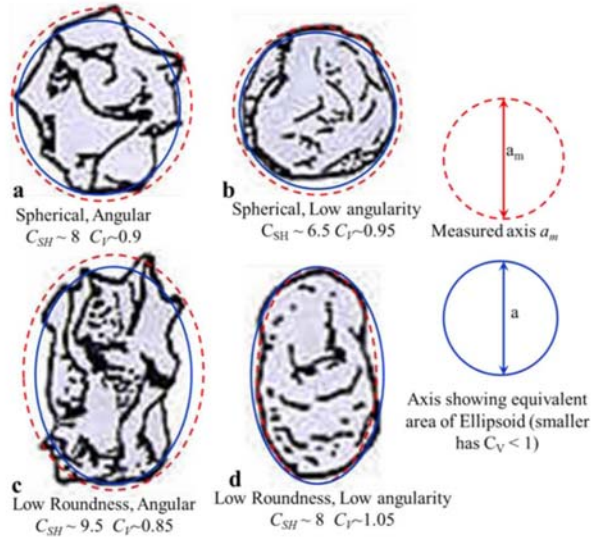
$$\eta = \eta_0 \exp\left(-\frac{\omega t}{2}\right) \left[ \cos\left(t \sqrt{\frac{g}{L_E} - \frac{\omega^2}{4}}\right) + \frac{\sin\left(t \sqrt{\frac{g}{L_E} - \frac{\omega^2}{4}}\right)}{\sqrt{\omega^2 L_E - 1}} \right]$$

- $\omega$  expresses head losses and  $K$  which dampen head ( $h$ )
- $L_E$  expresses velocity throughout permeameter (affected by  $\tau$ ) which control the time period ( $t_C$ )



# Surface area

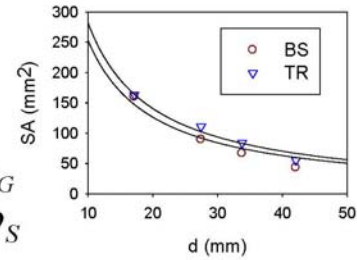
- Select grains were **measured** along the three axes to determine the axes of an ellipsoid with **equivalent volume** ( $C_V$ ).
- The perimeter of the three cross-sections were photographed and traced, then divided by the perimeter of an equivalent ellipse, providing the angularity ( $C_A/6$ ).
- The surface area of the ellipsoid was multiplied by  $C_V$  and  $C_A/6$  to give the surface area of the selected grain.
- The surface area per gram ( $SA_G$ ) was calculated for the larger grain size groups and used to calibrate  $C_{SH}$



$$SA_G = SA / g$$

$$SA = \sum_d (SA_G) m_G$$

$$C_{SH} = SA_G d_{eff} \rho_S$$





## The Kozeny-Carman Equation

- The Kozeny-Carman equation (KC eq.) was used with  $n$ ,  $SA$  ( $C_{SH}$  and  $d_{eff}$ ) and additionally  $\tau$  as suggested by Scheidegger (1957) and paired with the measured permeability values that are more precise and accurate than most data in the literature.
- $\tau$  has been theoretically investigated without conclusive results, it is evaluated here within  $C_{PK}$ .
- The KC eq. was used to empirically determine  $C_{PK}$  which was observed to increase by a factor of the tortuosity cubed for these tests as well as select results from Judge et al. (2013) that have different tortuosity values.
- Estimates within three times of  $K$  are accepted as a good grain-size analysis.

$$k = \frac{n^3}{(1-n)^2} \left( \frac{d_{eff}^2}{C_{SH}^2 C_{PK}} \right)$$

$C_{SH} = 6-9$  for spheres

$C_{PK} = 5$  for spheres

$\tau$  effects are usually ignored

(assumed to be 1)

- The packing factor  $C_{PK} = 5-10$  for specimens more tortuous than spheres where  $\tau = 1.06$
- $C_{PK}$  is back calculated using the measured ( $K_m$ ).

## The Packing Factor

$$C_{PK} = \frac{n^3}{(1-n)^2} \left( \frac{d_{eff}^2}{C_{SH}^2 k_m} \right)$$

$$C_{PK} = 5\tau^\eta \quad \eta \sim 3$$

•  $C_{PK}$  appears to be a function of  $\tau^\eta$  where  $\eta$  is theoretically 2 for inclined pipes (Costa 2006) as it is for gas flow through dry soil (Moldrup et al. 2004).

• There is no major trend in  $\eta$  for different  $\tau$  values but it averages 3.3 and is lower for the marbles.

• The believed reason for  $\eta$  values higher than 2 is the variability within the specimens that cause variability in the flow that may differ between specimens.

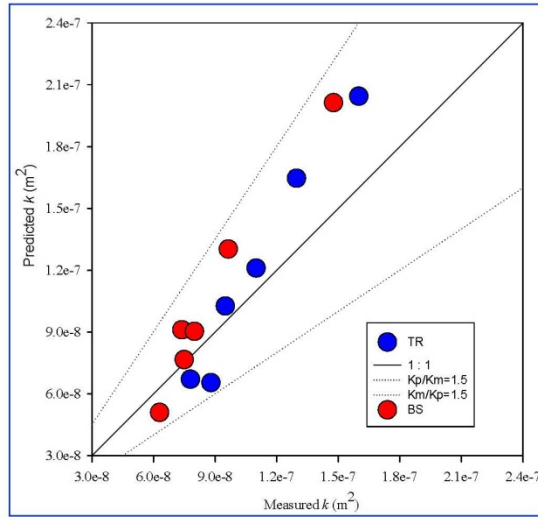
	A	B	C	D	E	F	G	H	I	
1		$d_{eff}$ (mm)	$n$ (-)	$(V_{ss}/SA)$ (mm <sup>-1</sup> )	$\tau$ (-)	$\eta$	$k_m$ (m <sup>2</sup> )	$k_p$ (m <sup>2</sup> )	$\delta$ ( $k_p/k_m$ )	
2	BS Big well graded	24	0.37	2.8	1.29	3.8	7.4E-08	9.1E-08	1.23	
3	BS Big skew graded	22	0.37	2.9	1.14	4.6	9.6E-08	1.3E-07	1.35	
4	BS Big uniform	21	0.42	3.1	1.27	4.3	1.5E-07	2.0E-07	1.36	
5	BS Small well graded	16	0.38	2.1	1.39	2.3	6.3E-08	5.1E-08	0.81	
6	BS Small skew graded	16	0.39	2.2	1.26	3.1	7.5E-08	7.7E-08	1.02	
7	BS Small uniform	16	0.40	2.3	1.28	3.5	8.0E-08	9.0E-08	1.13	
8	TR Big well graded	24	0.38	2.5	1.21	3.4	9.5E-08	1.0E-07	1.08	
9	TR Big skew graded	22	0.40	2.7	1.14	4.8	1.3E-07	1.6E-07	1.27	
10	TR Big uniform	22	0.42	2.8	1.20	4.4	1.6E-07	2.0E-07	1.28	
11	TR Small well graded	16	0.39	1.9	1.24	1.6	8.8E-08	6.5E-08	0.74	
12	TR Small skew graded	16	0.40	2.0	1.28	2.4	7.8E-08	6.7E-08	0.86	
13	TR Small uniform	16	0.42	2.0	1.13	3.8	1.1E-07	1.2E-07	1.10	
14	<i>Judge et al. (2013)</i>									
15	marbles	15	0.35	2.5	1.06	1.7	1.1E-07	1.2E-07	1.10	
16	V Stones	15	0.41	5.6	1.54	3.1	3.2E-07	3.4E-07	1.06	
17	H Stones	15	0.41	5.6	2.22	2.4	1.8E-07	1.1E-07	0.63	
18									Average:	0.89
19	BS $C_{SH}$ =	6.8							Standard Deviation:	0.22
20	TR $C_{SH}$ =	7.6							Relative Standard Deviation:	0.25



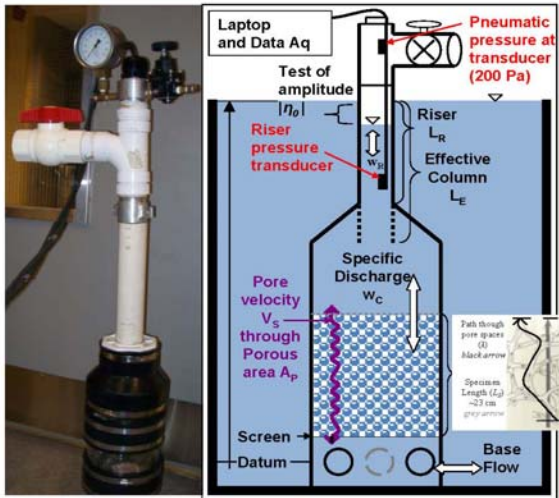
## Results and Conclusions

- The permeability is originally predicted more than twice as high as the measured with  $C_{PK} = 5$  for specimens of high tortuosity - noticeably the anisotropic stones, and not the marbles.
- The consideration of the tortuosity cubed in the packing factor provides  $k$  within an absolute factor of 1.4 of the measured value, an average of 1.2, and relative standard deviation of 0.25.
- The surface area method described in this study was found to yield  $C_{SH}$  values that are very close to the approximations given by Fair and Hatch (1933) (6.8 for BS, 7.6 for TR)
- The angularity lowers  $k$  but results in a higher void ratio which has a stronger effect on  $k$ .

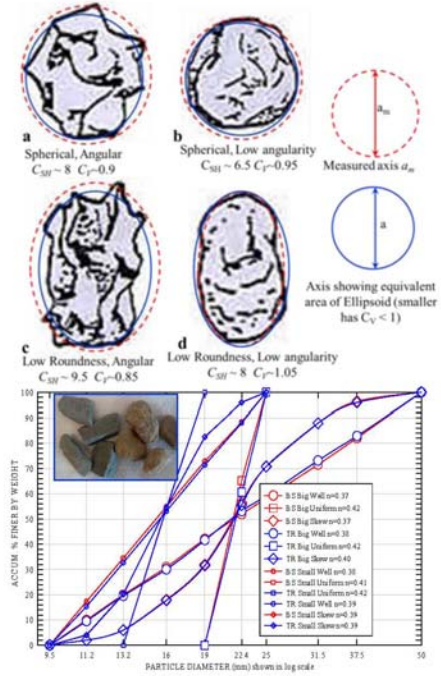
		BS $d_{eff} = 16$ mm	BS $d_{eff} = 23$ mm	TR $d_{eff} = 16$ mm	TR $d_{eff} = 23$ mm
Well graded	$K = (m/s)$	0.26	0.57	0.43	0.71
	$n =$	0.375	0.367	0.392	0.380
	$\tau =$	1.39	1.29	1.24	1.21
Curve graded	$K = (m/s)$	0.49	1.11	0.44	1.22
	$n =$	0.389	0.374	0.399	0.398
	$\tau =$	1.26	1.14	1.28	1.14
Uniform graded	$K = (m/s)$	0.57	1.28	0.90	1.43
	$n =$	0.405	0.416	0.416	0.420
	$\tau =$	1.28	1.27	1.13	1.20



# Thank you – Questions?



Judge, A., Ostendorf, D.W., DeGroot, D.J. and Zlotnik, V.A. (2013). “A Pneumatic Permeameter for Transient Laboratory Tests.” *Journal of Hydrologic Engineering. In Press.*



MassDOT, Highway Division, funded this research under Interagency Services Agreement 56565. The views, opinions, and findings contained in this document are the Author's and do not necessarily reflect the official view or policies of MassDOT.

## BIBLIOGRAPHY

- American Society for Testing and Materials (ASTM) D2434 "Standard test method for permeability of granular soils (constant head)" (2002). Annual Book of Standards, Volume 04.10, ASTM, West Conshohocken, Pennsylvania.
- Beveridge, G.S.G. and Schechter, R.S. (1970). *Optimization: Theory and Practice*. New York: McGraw Hill.
- Black, J.H. (2010). "The practical reasons why slug tests (including falling and rising head tests) often yield the wrong value of hydraulic conductivity." *Q. J. Eng. Geol.*, (43) 345-358.
- Bobo, A. M., Khoury, N., Li, H and Boufadel, M.C. (2012). "Groundwater Flow in a Tidally Influenced Gravel Beach in Prince William Sound, Alaska." *J. Hydrol. Eng.*, 17(4), 478-494.
- Bouwer, H. and Rice, H. C. (1976). "A slug test for determining hydraulic conductivity of unconfined aquifers with completely or partially penetrating wells." *Water Resour. Res.*, 12(3), 423-428.
- Butler, J.J. and Healey, J.M. (1998). "Relationship between pumping test and slug-test parameters: scale effect or artifact?" *Ground Water*, 36(2), 305–313.
- Butler, J.J. (1997). *The design, performance, and analysis of slug tests*. Lewis Publishers, Boca Raton, FL. 252 pp.
- Carman, P. C. (1956). *Flow of gases through porous media*. Butterworths Scientific Publications, London.
- Carrier, D. (2003). "Goodbye Hazen; Hello Kozeny-Carman." *Journal of Geotechnical and Geoenvironmental Engineering* 129(11), 1054-1056.
- Cedergren, Harry R. (1977). *Seepage, drainage and flow nets*. John Wiley and Sons, New York.
- Chapuis, R. P. and Aubertin M. (2003). "On the use of the Kozeny–Carman equation to predict the hydraulic conductivity of soils." *Can. Geotech. J.* 40: 616–628.
- Costa, A. (2006). "Hydraulic conductivity-porosity relationship: a re-examination of the Kozeny-Carman equation based on fractal pore-space geometry." *Geophys. Res. Lett.*, Vol. 33, L02318.
- Esling, S.P. and Keller, J.E. (2009). "A user interface for the Kansas Geological Survey slug test model." *Ground Water*, 47(4), 587-590.

- Fair, G. M. and Hatch, L. P. (1933). "Fundamental factors governing the stream-line flow of water through sand." *J. Am. Water Works Assoc.*, 25, 1551–1565.
- Ferreira, J. F., Ritzi, W. R. and Dominic, D. F. (2010). "Measuring the permeability of Open-framework gravel." *Ground Water*, 48(1), 87-101.
- Freeze, R. A. and Cherry, J. A. (1979). *Groundwater*. Prentice-Hall, Inc., Englewood Cliffs, NJ. 604 pp.
- Hamamoto, S., Moldrup, P., Kawamoto, K. and Komatsu, T. (2012). "Maxwell's Law Based Models for Liquid and Gas Phase Diffusivities in Variably-Saturated Soil." *Soil Sci. Soc. A, J.* 76, 1509-1517.
- Hyder, Z., Butler, J.J., McElwee, C.D. and Liu, W. (1994). "Slug tests in partially penetrating wells." *Water Resour. Res.*, 30(11), pp. 2945-2957.
- Judge, A.I., Ostendorf, D.W., DeGroot, D.J. and Zlotnik, V.A. (*in press*, 2013). "A Pneumatic Permeameter for Transient Laboratory Tests." *Journal of Hydrologic Engineering*.
- Lambe, T. W. and Whitman, R. V. (1969). *Soil Mechanics*. John Wiley and Sons Inc., New York.
- LaMesa, D. F. (2008). "Hydrogeologic Characterization of a Complex Geolacustrine Deposit in Eastern Massachusetts." University of Massachusetts, Amherst, MA." Master's thesis.
- Matyka, M., Khalili, A. and Koza, Z. (2008). "Tortuosity-porosity relation in the porous media flow". *Phys. Rev. E* 78, 026306.
- Moldrup, P., Olesen, T., Yoshikawa, S., Komatsu, T. and Rolston, D. E. (2004). "Three-Porosity Model for Predicting the Gas Diffusion Coefficient in Undisturbed Soil." *Sci. Soc. A, J.* 68, 750-759.
- NAVFAC (Naval Facilities Engineering Command) (1986). *NAVFAC design manual 7 – Soil mechanics, foundations, and earth structures*. Washington, DC: US Government Printing Office.
- Novakowski, K. (1989a). "Analysis of pulse interference tests." *Water Resour. Res.* 25(11), 2377-2387.
- Novakowski, K. (1989b). "A composite analytical model for analysis of pumping tests affected by wellbore storage and finite-thickness skin." *Water Resour. Res.* 25(9), 1937-1946.

Ostendorf, D.W., DeGroot, D.J. and Dunaj, P.J. (2007). "Waterhammer dissipation in pneumatic slug tests." *Water Resour. Res.*, 43(2), W02413.

Ostendorf, D.W., DeGroot, D.J., Dunaj, P.J. and Jakubowski, J. (2005). "A closed form slug test theory for high permeability aquifers." *Ground Water*, 43(1), 87-101.

Peres, A.M., Onur, M. and Reynolds A.C. (1989). "A new analysis procedure for determining aquifer properties from slug test data." *Water Resour. Res.*, 25(7), 1591-1602.

Plain, G. J. and Morrison, H. L. (1954). "Critical Reynolds number and flow permeability." *American Journal of Physics*, 22(3), 143-146.

Prats, M. and Scott, J.B. (1975). "Effect of wellbore storage on pulse test pressure response." *J. Pet. Tech.* 27(6), 707-709.

Scheidegger, A. E. (1957). *The physics of flow through porous media*. Macmillan, New York.

Spane, F. A. (1996). "Applicability of slug interference tests for hydraulic characterization of unconfined aquifers: (1) Analytical assessment." *Ground Water*, 34(1), 66-74.

Tennakoon, N, Indraratna, B., Rujikiatkamjorn, C., Nimbalkar, S., and Neville, T. (2012). "The role of ballast fouling characteristics on the drainage capacity of rail substructure." *ASTM Geotechnical Testing Journal*, 35(4), GTJ104017.

Trani, L. D. O and Indraratna, B. (2009). "The use of particle size distribution by surface area method in predicting the saturated hydraulic conductivity of graded granular soils." *Geotechnique*, 60(12), 1-6.

White, D. J., Vennapusa, P., Suleiman, M.T. and Jahren, C.T. (2007). "A device for rapid determination of permeability for drainable bases." *Geotechnical Testing Journal*, 30(4), ASTM, 1-10.

Zlotnik, V.A. and McGuire, V.L. (1998). "Multi-level slug tests in highly permeable formations: 1. Modification of the Springer-Gelhar (SG) model," *J. of Hydrology*, v. 204, 271-282.

Zurbuchen, B. R., Zlotnik, V. A. and Butler, J.J. (2002). "Dynamic Interpretation of Slug Tests in Highly Permeable Aquifers." *Water Resour. Res.*, 38(3), 7-1 - 7-18.